10.1161/CIRCULATIONAHA.117.030423

Inhibition of JAK-STAT Signaling Suppresses Pathogenic Immune Responses in Medium and Large Vessel Vasculitis

Running Title: *Zhang et al.; JAK/STAT Signaling in Vessel Wall Inflammation*

Hui Zhang, MD, PhD[1], Ryu Watanabe, MD, PhD[1], Gerald J. Berry, MD[2], Lu Tian, PhD[3], Jörg J. Goronzy, MD, PhD[1], Cornelia M. Weyand, MD, PhD[1*]

[1]Department of Medicine, Division of Immunology and Rheumatology; [2]Department of Pathology; [3]Department of Biomedical Data Science, Stanford University School of Medicine, Stanford, CA

[*]**Address for Correspondence**
C. M. Weyand, MD, PhD
Department of Medicine
Stanford University School of Medicine
CCSR Bld. R2225, 269 Campus Drive West
Stanford, CA 94305-5166, USA
Tel: 650-723-9027
Fax: 650-721-1251
Email: cweyand@stanford.edu.

Abstract

Background—Giant cell arteritis (GCA), a chronic autoimmune disease of the aorta and its large branches, is complicated by aneurysm formation, dissection, and arterial occlusions. Arterial wall dendritic cells (DC) attract $CD4^+$ T-cells and macrophages (Mo), to form prototypic granulomatous infiltrates. Vasculitic lesions contain a diverse array of effector T-cells that persist despite corticosteroid therapy and sustain chronic, smoldering vasculitis. Transmural inflammation induces microvascular neoangiogenesis and results in lumen-occlusive intimal hyperplasia. We have examined whether persistent vessel wall inflammation is maintained by lesional T-cells, including the newly identified tissue-resident memory T cells (T_{RM}) and whether such T-cells are sensitive to the cytokine signaling inhibitor tofacitinib, a JAK inhibitor (Jakinib) targeting the Janus kinase (JAK) 3 and JAK1.

Methods—Vascular inflammation was induced in human arteries engrafted into immunodeficient mice that were reconstituted with T-cells and monocytes from GCA patients. Mice carrying inflamed human arteries were treated with tofacitinib or vehicle. Vasculitic arteries were examined for gene expression (RT-PCR), protein expression (immunohistochemistry) and infiltrating cell populations (flow cytometry).

Results—Tofacitinib effectively suppressed innate and adaptive immunity in the vessel wall. Lesional T-cells responded to tofacitinib with reduced proliferation rates (<10%) and minimal production of the effector molecules IFN-γ, IL-17 and IL-21. Tofacitinib disrupted adventitial microvascular angiogenesis, reduced outgrowth of hyperplastic intima and minimized $CD4^+CD103^+$ tissue-resident memory T-cells.

Conclusions—Cytokine signaling dependent on JAK3 and JAK1 is critically important in chronic inflammation of medium and large arteries. The Jakinib tofacitinib effectively suppresses tissue-resident memory T-cells and inhibits core vasculitogenic effector pathways.

Key Words: vasculitis; cytokine; cell signaling; giant cell arteritis, T cell

Clinical Perspective

What is new?

- STAT1 and STAT2 target genes, the transcription factors STAT1 and STAT2 and the STAT-pathway activators type I and type II interferon are abundant in the tissue transcriptome of arteries with GCA.
- The JAK/STAT inhibitor Tofacitinib suppresses the ex-vivo induction of IFN-□□ T-cells in GCA patients.
- Chimeric mice carrying human arteries and immune cells from GCA patients develop persistent vasculitis.
- In the chimeras, Tofacitinib efficiently suppresses T-cell invasion into the artery, inhibits proliferation and cytokine production of vasculitogenic T-cells and curbs survival of artery-resident T-cells.
- Tofacitinib treatment prevents neoangiogenesis and intimal hyperplasia in inflamed arteries.

What are the clinical implications?

- The JAK/STAT inhibitor Tofacitinib effectively targets multiple disease-relevant processes in inflammatory vasculopathy and represents a potential disease-modifying agent.

Introduction

Vasculitides of large elastic arteries are infrequent, but potentially fatal diseases, damaging vital blood vessels, such as the aorta, the subclavian-axillary bed, the carotid branches, and mesenteric arteries. Giant cell arteritis (GCA) accounts for most cases of autoimmune large vessel vasculitis; typically causing vision loss, aortic arch syndrome, aortic dissection, and aortic aneurysms. Extravascular GCA, consistent of an intense hepatic acute phase response (APR) gives rise to highly elevated laboratory markers of inflammation. Whether the hepatic APR precedes or follows vascular inflammation is unresolved. GCA is a chronic condition, which persists despite long-term therapy with high-dose corticosteroids[1,2] and disease risk genes have been localized to multiple biologic pathways[3].

$CD4^+$ T-cells and macrophages dominate the transmural lesions of this granulomatous vasculitis. Arterial wall dendritic cells (DC) function as gatekeepers and by providing access to invading T-cells and macrophages fail to protect the artery's immune privilege[4,5]. In GCA arteries, wall-resident DC express low concentrations of the immunoinhibitory ligand PD-L1, disarming the protective PD-1 immune checkpoint[6,7]. Tissue-infiltrating $CD4^+$ T-cells are $PD\text{-}1^+$, yet are highly activated, non-exhausted and cover multiple effector functions. Most prominent are tissue Th1 and Th17 cells, but IL-21- and IL-9-producing T-cells are also present[8,9]. Heterogeneous T-cell effector populations in the lesions are indicative of an unopposed T-cell response.

GCA's chronicity suggests a role for tissue-resident memory T-cells (T_{RM}), a recently discovered T-cell lineage residing in tissues, where they provide fast and powerful helper functions[10]. Different from central memory and effector memory T-cells, T_{RM} cells receive localizing signals in the tissue niche and do not recirculate to secondary lymphoid organs. Two

phenotypic markers, CD69 and CD103 (a receptor recognizing E-cadherin), have been identified[11]. T_{RM} cells in E-cadherin^{low} tissues lacking epithelium possibly express alternative markers, such as type I collagen receptors. Originally considered crucial for rapid anti-pathogen responses, T_{RM} cells may also drive autoimmune tissue inflammation[12]. Functional heterogeneity, being able to release IFN-γ, IL-17, IL-9, and TNF-α, enables pro-inflammatory effector functions of T_{RM} cells[13]. Tissue-derived IL-7, IL-15 and TGF-β are believed to guide T_{RM} recruitment, differentiation and maintenance[13]. Whether T_{RM} are involved in building and sustaining GCA's granulomatous lesions and the arterial wall remodeling process is unknown.

T-cells depend on signals through their T-cell receptor (TCR), but require input from the cytokine milieu to direct their clonal expansion, persistence, and functional differentiation. Environment-cell communications rely on cytokine signals that trigger the Janus kinase (JAK) and signal transducer and activator of transcription (STAT) pathway[14]. The JAK/STAT signaling pathway has been implicated in cancer cell growth and autoimmunity[15]. Th1 lineage commitment is strictly linked to STAT1- and STAT4-mediated gene induction[16]. STAT3 is considered the master regulator for Th17 cell differentiation. Gene polymorphisms encoding type I cytokine receptors and their signaling elements (IL-23R, IL-12B, JAK2 and STAT3) are linked to inflammatory bowel diseases and psoriasis[17]. STAT4 polymorphisms are associated with rheumatoid arthritis (RA), Sjogren's syndrome and systemic lupus erythematosus[18,19]. JAK/STAT's critical role in immune-mediated disease has been therapeutically exploited with the development of Jakininbs, small molecule inhibitors that block the action of type I/II cytokines. The JAK3/1 inhibitor Tofacitinib[20] has been approved for RA treatment[21]. JAK3-activating mutations in T-cell acute lymphoblastic leukemia and JAK3-inactivating mutations in severe immunodeficiency emphasize the critical role of JAK3 in T-cell biology[22,23]. Most

prominently, JAK3 inactivation results in loss-of-function of the common gamma chain (γc); causing X-linked severe combined immunodeficiency[23,24]. Cytokines central in regulating T-cell activation and survival (IL-2, IL-4, IL-7, IL-9, IL-15, IL-21) all employ JAK3 to mediate their effect[25].

Chronic GCA requires T-cells persisting in the arterial wall; to orchestrate macrophage activation, drive inflammation-associated neo-angiogenesis and promote intimal hyperplasia[26,27]. Current therapies focus on pro-inflammatory innate cytokines[28,29], but fail to eliminate wall-infiltrating T-cells[2]. We have explored whether targeting JAK3 with the JAK inhibitor (Jakinib) tofacitinib can remove disease-relevant T-cells from inflamed arteries. To overcome limitations in examining in-situ T-cells, we have employed a human-artery SCID chimera model, in which vascular inflammation is induced in engrafted human arteries by reconstituting such chimeras with peripheral blood mononuclear cells (PBMCs) from GCA patients[6,30]. In this model system, alloantigens serve as model antigens to probe immunoregulatory defects in GCA patients that are relevant for immune responses in the microenvironment of the vessel wall. Tofacitinib therapy was highly effective in suppressing vasculitogenic immunity by inhibiting the clonal expansion of wall-residing T-cells. Processes downstream of vasculitogenic T-cell activity, e.g. microangiogenic growth of capillary networks and intimal hyperplasia were effectively disrupted. Most importantly, we demonstrate the existence of tissue-anchored $CD4^+$ $CD103^+$ T-cells in chronically inflamed arteries. Keeping such $CD103^+$ T_{RM} cells alive and functional required JAK/STAT signaling and was successfully inhibited in tofacitinib-treated chimeras. Selective Jakinibs may provide new avenues to manage acute and chronic large vessel vasculitis.

Methods

All data supporting this study's findings are available from the corresponding author upon request.

Patients and tissue samples

Temporal arteries were collected from diagnostic biopsies. GCA was diagnosed based on typical histologic findings[2]. Noninflamed human axillary arteries free of wall-infiltrating T-cells and macrophages derived from tissue donors (12-18 hours postmortem). Patients with a tissue diagnosis of GCA and active disease donated blood for the study. The Stanford Blood Bank Research Program supplied age and sex-matched healthy controls. Pre-existing cancer, autoimmune disease, or chronic viral infection were exclusion criteria. Clinical characteristics of the study patients are summarized in Table 1.

PBMCs were isolated by density-gradient centrifugation (Lymphoprep, Oslo, Norway). Naïve $CD4^+$ T-cells were purified by negative selection (EasySep™ naïve $CD4^+$ T-Cell enrichment kits, STEMCELL Technologies, Vancouver, BC, Canada).

Human Artery-Severe Combined Immunodeficiency Mouse Chimeras

NOD.Cg-Prkdcscid Il2rgtm1Wjl/SzJ (NSG) mice were purchased from Jackson Laboratory (Sacramento, CA). Human artery-mouse chimeras were generated as published[6,31]. Normal temporal or axillary arteries were cut into rings (3 mm) and engrafted into a midline subcutaneous pocket of the mice. Six days later, mice received 10 µg LPS. The next day, PBMCs (1×10^7) from a patient with active GCA or an age-matched healthy individual were adoptively transferred into each mouse.

For model validation we compared induction of vessel wall inflammation after transfer of PBMC from age-matched controls or GCA patients into artery-engrafted NSG mice

(Suppl.Fig.1). Transferred human cells establish organized lymphoid structures in the murine spleen[32]. Spleen/body weight ratios were similar in mice receiving control or patient-derived PBMC (Suppl.Fig.1A); indicating similar immuno-reconstitution of paired mice carrying the same arterial tissue, but receiving healthy or GCA PBMC. Numbers of transferred human cells were chosen such that allogeneic recognition of arterial cells was avoided. To detect even subtle inflammation in the artery grafts, marker gene transcripts were monitored in the tissue transcriptome of explanted grafts (n=10 each from control PBMC or GCA PBMC-reconstituted mice). Based on tissue transcripts for the monocyte/macrophage marker CD163 and the DC marker CD83, only patient-derived PBMC were successful in inducing inflammation (Suppl.Fig.1B, C). As expected, arterial grafts were free of transcripts for TCR, T-bet and IFN-□ in the absence of human PBMC. No signal for tissue-infiltrating T-cells was recorded in mice reconstituted with control PBMC, but GCA-PBMC produced robust T-cell infiltrates (Suppl.Fig.1D). VEGF is an excellent marker of endothelial cell activation and neoangiogenesis in GCA[31]. Tissue VEGF transcripts were indistinguishable in grafts from PBMC-free mice and control-PBMC-reconstituted mice, but were upregulated in the presence of patient-derived PBMC (Suppl.Fig.1E).

To examine the impact of the artery graft on immune reconstitution, NSG mice were assigned to parallel treatment arms: Arm 1 received an artery as in Suppl.Fig.1; Arm 2 was sham operated. Mice were immune-reconstituted with $1x10^7$ GCA PBMC. Immune reconstitution was assessed after 7 days in the chimeras' spleen and circulating blood. Human T-cells were quantified by flow cytometry of $CD45^+CD3^+$ cells (Suppl.Fig.2).

Tofacitinib treatment

Mice carrying arterial tissue from the same donor and immuno-reconstituted with PBMCs from the same patient were randomly assigned to the vehicle or tofacitinib-treatment group. Tofacitinib dosing was assessed in pilot experiments to avoid T-cell and monocyte cytopenia[33]. In experiments shown here, mice received 3 mg/kg tofacitinib or equal volume of vehicle orally daily over one to two weeks as indicated[34]. Grafts were harvested at the end of the experiment, snap-frozen for RNA isolation or OCT-embedded for H&E and immunostaining. To prepare single-cell populations, explanted spleens or arteries were minced into pieces and incubated with collagenase I (2 mg/ml) and Dnase (40 U/ml) at 37°C. Cells were filtered through a cell strainer to prepare single-cell suspensions.

Statistics

Statistical analysis was performed using GraphPad Prism 5.0. All data are expressed as mean±SEM and $p<0.05$ was considered statistically significant. Populations were compared using t-test or Wilcoxon test as appropriate. To adjust for multiple testing, in addition to individual p-values, we used Hochberg's step-down method to control for a family-wise-error rate at the 0.05 level. To assess interventions, we applied paired t-test or paired Wilcoxon test. The Wilcoxon test was used for robustness when the sample size per group was >5. Where appropriate, one-way ANOVA was used and pair-wise comparison using Tukey's method to adjust for multiple testing was applied.

Study approval

All procedures and biospecimen collections were approved by the Institutional Review Board and informed consent was obtained as appropriate. The animal protocol was approved by the Animal Care and Use Committee.

Additional methods available in the supplementary file. PCR primers are listed in Suppl. Table 1.

Results

Expression of STAT target genes in GCA-affected arteries

Temporal arteries with the typical granulomatous lesions of GCA are a cytokine-rich tissue environment[35], with a multitude of innate and adaptive effector molecules. Th1-cell derived IFN-γ is a critical disease driver[36,37], but less is known about tissue concentrations of other adaptive and innate cytokines, including IL-21, IL-1, IL-6 and TNF-α. In search for clues which cytokines may be key activators in GCA arteries, we made use of the fact that many cytokines signal through JAK/STAT pathways to mediate their pro-inflammatory functions. To support the concept that selected JAK-STAT signaling pathways are particularly relevant for GCA inflammation, we evaluated the expression of selected STAT target genes (Fig.1A). STAT1- and STAT2-dependent target genes (T-bet, CXCL9, ISG15, OAS1) were strongly upregulated in the vasculitic arteries. Target genes induced by STAT3, STAT5a and STAT6 signaling were consistently low; indistinguishable from normal, noninflamed temporal arteries (Fig.1A). Typically, each of the STAT family members is a target gene induced when the respective transcription factor is activated[17]. Thus, we quantified transcripts for STAT1, STAT2, STAT3, STAT4, STAT5a and STAT6 in 8 diagnostic biopsies from GCA-affected and 8 noninflamed specimens (Fig.1B-1G). Transcripts for all STAT family members were at low abundance in normal arteries and STAT3, STAT5a and STAT6 remained sparsely expressed in GCA-affected arteries. In contrast, STAT1, STAT2 and STAT4 transcripts were abundantly present in vasculitic arteries (Fig.1B-1D). After adjustment for multiple testing using the Benjamini–Hochberg method, the STAT1 increase remained statistically significant. STAT1 and STAT2 are

the key transcription factors triggered by interferons; with type 1 interferons activating STAT1/2 heterodimers and IFN-γ activating STAT1 homodimers[38]. We examined the tissue transcriptome of noninflamed and inflamed arteries for IFN-α, IFN-β and IFN-γ transcripts (Fig.1H-1J) and found significantly elevated concentrations of IFN-α and IFN-γ specific sequences; suggesting that both type I and II interferons are actively participating in the vasculitic lesions. The STAT4 target gene furin and STAT4 transcripts were borderline elevated in vasculitic versus normal arteries. Target genes for STAT3 and STAT6 were distinctly low; questioning a role for IL-6 and IL-4 in the tissue microenvironment. The STAT5 target gene FoxP3 was barely detectable in the tissue transcriptome.

Albeit providing only indirect evidence, these gene expression data suggested predominance of STAT1 and STAT1/2 activation events in GCA lesions, focusing attention onto type I and type II interferons.

IFN-γ production in GCA T-cells is susceptible to the JAK/STAT inhibitor tofacitinib

Considering the predominance of STAT1 in the vasculitic infiltrates, we explored whether $CD4^+$ T-cells from GCA patients are biased towards IFN-γ production and whether Th1 lineage commitment involves JAK3 activation. We stimulated $CD4^+$ T-cells from patients and age-matched controls under non-skewing conditions and tested whether Th1 commitment was sensitive to the JAK3 inhibitor tofacitinib (Fig.2). As antigen-presenting cells were excluded from the cultures, stimulation conditions relied exclusively on T-cell receptor signaling. Tofacitinib preferentially suppresses signals dependent on cytokine receptors containing the γc chain (IL-2, IL-4, IL-7, IL-9, IL-15, IL-21)[39]. Over 6 days, an average of 18% of healthy $CD4^+$ T-cells became IFN-γ producers. Tofacitinib (30 nM) decreased the proportion of Th1-lineage-committed cells to 13%; indicating that one-third of the type II interferon-producing T-cells

depended on JAK/STAT-derived signals (Fig.2A, 2B). $CD4^+$ T-cells from GCA patients were spontaneously biased towards IFN-γ production. TCR activation induced intracellular IFN-γ stores in 25% of $CD4^+$ T-cells. A substantial proportion of these cells were susceptible to JAK/STAT inhibition, which reduced frequencies of IFN-γ^+ $CD4^+$ T-cells to 15 % (Fig.2A, 2B).

These data indicated that GCA patients guide $CD4^+$ T-cells towards Th1 effector functions, specifically IFN-γ production, and that pharmacologic inhibition of JAK3/1 effectively suppresses this abnormality.

Tofacitinib inhibits inflammatory responses in the vessel wall

To investigate whether the pathogenic immune responses leading to vascular inflammation depend on γc-containing cytokine receptors, inflammation was induced in human arteries engrafted into NSG mice by immunoreconstituting such mice with PBMCs from GCA patients (Fig.3).

Vessel wall infiltrates were markedly reduced in tofacitinib-treated grafts (Fig.3A). Especially, the density of tissue-infiltrating $CD3^+$ T-cells declined. The concentration of TCR transcript was consistently lower after blockade of γc-chain–containing cytokine receptors. In a series of 8 independent experiments, numbers of tissue-residing T-cells reached 51.00±6.2/high-powered field and declined to 22.7±3.3/high-powered field in tofacitinib-treated mice (Fig.3B, 3C). Tofacitinib's T-cell–depleting effect was examined by enumerating T-cell counts in single-cell preparations extracted from digested arteries (Suppl.Fig.3). Resembling GCA-affected temporal arteries, $CD4^+$ T-cells dominated the wall infiltrates and tofacitinib reduced the number of tissue-infiltrating CD4 and CD8 T-cells by about 80%. The immunosuppressive effect of the JAK3/1 inhibitor was not limited to T-cells. With reduced T-cell accumulation in the tissue, tissue macrophages declined as well; as indicated by the consistently lowered expression of the

macrophage marker CD163 (Fig.3D). We examined whether JAK3/1 blockade affected recruitment and retention versus in situ expansion of tissue-infiltrating T-cells (Fig.3E, 3F). Tissue-residing T-cells were highly proliferative in vehicle-treated arteries. About 40% of tissue-residing CD3 T-cells expressed the proliferation marker Ki-67, suggesting that clonal expansion contributes significantly to the formation of the intramural lesions. As JAK3-dependent signaling was disrupted with tofacitinib treatment, <10% of tissue-entrapped T-cells were dividing (Fig.3F). Tofacitinib's anti-proliferative effect was not restricted to T-cells recruited to the vessel wall. Human T-cells in the blood and in the murine spleen also declined, implicating γ-chain$^+$ cytokine receptors in homeostatic T-cell expansion in the murine host. Since the γc chain is mostly utilized by T-cell growth and differentiation factors (IL-2, IL-4, IL-7, IL-9, IL-15, IL-21), reduced frequencies of human CD14$^+$ monocytes in tofacitinib-treated mice may be the result of impaired T-cell–derived survival signals for these myeloid cells (Suppl.Fig.4A-4D).

To understand how suppression of T-cell growth affects T-cell effector functions at the site of tissue inflammation, we analyzed gene expression patterns for lineage-determining transcription factors (T-bet, RORC, Bcl-6, FoxP3) as well as transcripts for the T effector cytokines IFN-γ, IL-17 and IL-21. Th1, Th17 and Tfh cells have all been localized to the vasculitic lesions and have been implicated in tissue-damaging inflammation[40]. Tofacitinib treatment left expression of FoxP3 transcripts unaffected, but reduced concentrations of T-bet, RORC and BCL-6 by more than 40% (Fig.4). The immunosuppressive effect of the JAK3 inhibitor was even more pronounced for effector cytokines. IFN-γ and IL-17 mRNA was reduced to minimal levels and IL-21 mRNA declined by 58% (Fig.4).

Taken together, common γ-chain function appears critical in the pathogenic cascade of vascular inflammation and JAK1/3 inhibition effectively interferes with the expansion of granulomatous lesions and the pro-survival signals produced in the tissue microenvironment.

Tissue-resident memory T cells (T_{RM}) require JAK1/3 function to survive

T_{RM} have recently been recognized as a transcriptionally, phenotypically and functionally distinct lymphocyte lineage, distinct from classical memory T-cells[41]. Specialized to keep residency in the tissue microenvironment, T_{RM} are believed to provide fast and effective immune responses when reencountering antigens[11]. Expression of the alpha E integrin CD103, which combines with the integrin beta 7 to form the ligand for E-cadherin, has been mechanistically linked to tissue anchoring[42]. Given their persistence in peripheral tissues, T_{RM} are considered essential pathogenic elements in chronic inflammatory disease[10]. In support of the concept, that intramural vasculitic foci contain T_{RM}, we found that tissue-extracted T-cells included a population of $CD4^+CD103^+$ T-cells, that was essentially exclusively present in the arterial wall and was barely detectable in the peripheral blood (Fig.3G, 3H and Suppl.Fig.5). This population of CD4 T memory cells was highly sensitive to tofacitinib, implicating γc chain-signaling cytokines in its survival.

To further study T_{RM} in vasculitic lesions, we developed a transengraftment model, in which arterial inflammation was first induced in engrafted human arteries, before they were transplanted into an "empty" NSG mouse (Fig.5A). This model system avoided competition between continuous recruitment of new T-cell specificities into the vessel wall with T-cells residing and proliferating in the lesion. Following the removal from continuous T-cell supply, the arterial wall infiltrates maintained high proliferative activity, the density of tissue-invading T-cells grew and the expanding T-cell populations moved deeper into the vascular wall layers

(Fig.5B, 5C). A subset of 5-8% of T-cells acquired expression of the CD103 marker, as identified by flow cytometric analysis of cells isolated out of the human arteries (Fig.5G, 5H). About 25% of the tissue-residing T-cells were Ki-67 positive, identifying them as dividing cells (Figure 5E, 5F). Over a period of 2 weeks, the number of T-cells seen in tissue sections doubled (Fig.5C, 5D). Growth in the vasculitic infiltrates was associated with 2-3–fold increase in the expression of transcripts specific for T-bet, RORC, IFN-γ, IL-17 and IL-21 (Fig.5I). If the "empty" NSG mice engrafted with the already inflamed arteries were treated with a daily oral dose of tofacitinib (3 mg/kg), the density of tissue-infiltrating T-cells declined markedly, returning to levels seen in nontransplanted arteries (Fig.5C,5D). In parallel, accumulation of cytokine-producing T-cells was effectively stopped, as demonstrated by the marked reduction in T-bet, RORC, IFN-γ, IL-17 and IL-21 mRNA (Fig.5I). Most importantly, tofacitinib effectively disrupted survival signals for $CD4^+CD103^+$ T_{RM} cells, which sank to low frequencies in artery grafts treated with the jakinib (Fig.5G, 5H).

To examine whether the microenvironment of the inflamed arterial wall is permissive to support the induction and survival of T_{RM}, we searched for the presence of IL-7, IL-9 and IL-15 in the tissue microenvironment (Suppl.Fig.6), as these cytokines have been implicated in supporting T_{RM}[43]. Induction of vessel wall inflammation was associated with significant upregulation of IL-7, IL-9 and IL-15 (Suppl.Fig.6A-6C); supplying critical ingredients for local T-cell persistence and growth.

In essence, T_{RM} in the inflamed vessel wall require JAK3/1-dependent signaling to survive and inhibiting the kinase activity appears to be an effective strategy in halting vasculitogenic immune responses.

Jak3-STAT signaling drives inflammation-associated microangiogenesis in the inflamed vessel wall

When affected by GCA, large and medium arteries develop a dense network of microvessels, leading to adventitial thickening and giving rise to the enhancement effect on imaging studies[1]. Newly formed microvessels are identified by tissue stains for α-SMA–expressing pericytes and vWF^+ endothelial cells[6]. Adventitial vasa vasorum are present in healthy, noninflamed arteries (Fig.6A, left) and remained essentially unchanged, if arteries were engrafted into mice lacking patient PBMC (Fig.6A central, 6B). Induction of vasculitic wall infiltrates in PBMC-reconstituted chimeras was associated with robust neoangiogenesis (Fig.6A right, 6B), indicating the critical role of the donor immune cells in the process of neoangiogenesis. The numbers of microvessels identified by immunostaining in tissue sections were more than 10-fold higher in arterial grafts after successful induction of transmural inflammation (Fig.6B).

To explore whether γ-chain–dependent signaling had a role in this damage-associated pattern, chimeras with inflamed human arteries were assigned to a vehicle or a tofacitinib treatment arm (Fig.6C-6E). Grafts explanted from vehicle treated animals had dense networks of newly formed microvessels (Fig.6C) and tissue-extracted RNA contained high transcript levels for the angiogenic factors PDGF, FGF2 and VEGF (Fig.6E). Inhibition of JAK3 activity with tofacitinib robustly suppressed the neoangiogenic response. Numbers of microvessels were less than 50% of those in the vehicle control arteries (Fig.6C, 6D). Tissue concentrations of transcripts specific for PDGF, FGF2 and VEGF (Fig.6E) were strongly tofacitinib-responsive.

These experiments implicated signaling through the γc chain in the disease-relevant process of microangiogenesis, which supplies oxygen and nutrients to the thickening arterial wall and the expanding intimal layer. The Jakinib tofacitinib was sufficient to arrest the

neoangiogenic program, in support of a direct role for activated T-cells in the growth of new vasa vasora.

JAK1/3-STAT signaling promotes intimal hyperplasia

The ischemic complications of GCA, above all the ischemic damage to the optic nerve, result from arterial stenosis/occlusion, caused by fast and concentric intimal hyperplasia[44]. Induction of transmural inflammation in engrafted human arteries was associated with high proliferative activity in vascular cells, both in the media and the intima, leading to growth of the intimal layer (Fig.7A, 7B). Over a disease period of 2 weeks, the tunica intima grew to a thickness of 30-40 μm, equivalent to 15-20 cell layers. Proliferative activity was encountered in two cellular populations: (1) cells expressing the smooth muscle cell/fibroblast marker α-SMA, which were enriched in the adventitia and intima; (2) α-SMA^{neg} cells localized within the immune cell infiltrates and centering on the media (Fig.7C, 7D). Such proliferating α-SMA-negative cells represent T-cells and macrophages (Fig.3). Tofacitinib treatment essentially curbed the proliferative activity of all dividing cell populations (Fig.7C, 7D). The hyperplastic reaction of the intima was aborted, thickness measurements fell from 35 to 10 μm (Fig.7A, 7B). The anti-proliferative effect of tofacitinib equally affected α-SMA-expressing vascular cells and infiltrating immune cells; which may reflect direct and indirect inhibition of growth signals. Few dividing cells remained in the arteries treated with tofacitinib (Fig.7C, 7D).

These data connected γc chain cytokine responses to the damage pattern of intimal hyperplasia. Blocking Jak3-STAT signaling suppressed proliferative activity of immune and nonimmune cells, successfully protecting the vascular wall from inflammation-induced remodeling.

Discussion

GCA is a prototypical large vessel vasculitis, caused by vasculitogenic T-cells and macrophages building organized lymphoid microstructures in the otherwise immuno- privileged niche of the vessel wall. Long-lived T-cells coordinate effector functions of accompanying macrophages and vessel wall cells react with a maladaptive repair response, ultimately promoting vascular failure. Acutely, GCA is treated with high-dose corticosteroids, which suppress nonspecific innate immunity, but spare the multifunctional T-cells trapped in the lesions[2,40]. Persistent functional activity of lesional T-cells creates smoldering vasculitis, the ultimate challenge in the management of affected patients.

Here, we have characterized the proliferative capacity of the vasculitogenic T-cells and have identified $CD4^+CD103^+$ T_{RM} anchored in inflammatory wall lesions. $CD4^+CD103^+$ T_{RM} function as key drivers of long-lasting inflammation and represent preferred therapeutic targets to eradicate inflammatory vasculopathy. Tissue-resident and mobile $CD4^+$ memory T-cells both relied on survival signals through γc chain-containing cytokine receptors; as documented by the powerful immunosuppressive effects of the JAK1/3 inhibitor tofacitinib. The therapeutic effectiveness of this jakinib focusses attention towards cytokines binding type I and type II cytokine receptors, in particular interferons.

Early studies in GCA temporal arteries emphasized the sharing of T-cell receptor sequences in physically separated vasculitic foci, compatible with antigen driving lesional T-cells. However, the concept of a single vasculitogenic autoantigen has recently been replaced by a disease model that focusses on antigen-nonspecific defects driving vasculitis. The emerging paradigm recognizes broad immuno-regulatory defects in GCA, indicative of T cell hyperreactivity due to altered activation threshold setting. Hyperreactive T-cells in GCA patients

result from failed immune checkpoints that control the response to many antigens. Specifically, NOTCH1$^+$ CD4$^+$ T-cells in GCA patients receive activating signals from Jagged1$^+$ microendothelial cells in the arterial adventitia[31]. Also, a defect in the immunoinhibitory PD-1 checkpoint enables unopposed T-cell activity in the vascular lesions[6]. And, patients' CD4$^+$ T-cells are insufficiently suppressed due to the failure of immunoinhibitory CD8 Treg cells[45]. These data emphasize the importance of the tissue environment in enabling inappropriate T-cell immunity and reveal abnormalities in T cell responsiveness that are applicable to a broad spectrum of antigens. Which antigens are recognized in the human artery-SCID mice is not known, but alloantigens serve as model antigens to probe T-cell reactivity in GCA. Insufficient control of a broad range of adaptive immune responses in GCA patients appears best matched by therapeutically targeting the T cell's signaling machinery; in line with the anti-inflammatory effects of the JAK1/3 inhibitor tofacitinib demonstrated in the current study.

Several lines of evidence support the concept that interferons, including type I (IFN-α/β) and type II (IFN-γ) are of particular relevance in GCA. IFN-α/β and IFN-γ trigger JAK-STAT signaling, with both types of interferon activating STAT1[46]. STAT2 functions as a transcription factor for type I interferon-dependent responses[47]. The tissue transcriptome of GCA-affected arteries contained a signature indicative for in situ interferon responses: IFN-α and IFN-γ transcripts were significantly increased, target genes for STAT1 (T-bet, CXCL9) and STAT2 (ISG15, OAS1) were enriched and STAT1 and STAT2 were selectively upregulated; supporting the pinnacle role of T-cells in the disease process. The IFN-□–rich environment provides ideal conditions for highly activated and functionally diverse macrophages arranged in the typical granulomatous infiltrates[37] How this IFN-□–rich environment promotes other disease components, especially the formation of new blood vessels and the hyperplasia of the intima, is

more difficult to understand. The current paradigm holds that both types of interferon are anti-angiogenic. Previously, macrophages and multinucleated giant cells were identified as the producers of the angiogenic factor VEGF in GCA-affected temporal arteries[48]. Indeed, in temporal artery biopsies, tissue IFN-□ and VEGF were strongly associated with the degree of intramural vessel formation; demonstrating that in this vasculitis IFN-□ promotes and not suppresses neoangiogenesis[48].

Unexpectedly, STAT3 target genes were at low abundance in the temporal artery biopsies; questioning in-situ action of IL-6, which may mostly function in extravascular sites. Also, the low expression of STAT6 target genes is in line with a lack of IL-4 production in GCA lesions[49].

The current treatment paradigm in GCA is the use of corticosteroids, which preferentially target innate cytokines, such as IL-1β, IL-12 and IL-6[36], but have little effect on tissue-residing T-cells[2,36]. Therapeutic needs therefore lie in eliminating the T-cell infiltrates. Functionally, lesional T-cells are highly diverse[40], but data presented here indicate that they dependent on common survival signals. Inflamed arteries were rich in T-cell growth and survival cytokines (Suppl.Fig.6) and inhibiting the activity of JAK1/3 was sufficient to broadly diminish lineage-determining transcription factors (T-bet, RORC and BCL-6) and T-cell effector molecules (IFN-γ, IL-17 and IL-21). Tofacitinib minimized the in-situ proliferation of lesional T-cells and flow cytometric analysis confirmed that the T-cell suppressive effect of disrupting JAK-STAT signaling included $CD4^{+}CD103^{+}T_{RM}$. Tofacitinib's powerful immunosuppressive effect is encouraging, as it may be able to disrupt upstream pathogenic drivers and turn the disease from a long-lasting wall inflammation into an acute and treatable condition.

Tissue-resident memory T-cells (T_{RM}) have recently been described as a specialized T-cell subset defined by its exquisite ability to anchor in peripheral tissues instead of returning to

secondary lymphoid organs. For protective immunity, T_{RM} provide fast and locally effective protection. For vasculitogenic immunity, such T-cells may hold the key to chronicity and persistent wall injury, even after good control of peripheral inflammatory markers has been reached. We confirmed the tissue residence of $CD4^+CD103^+$ T-cells by transengrafting inflamed arteries into "empty" mice, making vascular lesions the sole reservoir for human cells. $CD4^+CD103^+$ T-cells were explicitly infrequent in the periphery, but populated the transmural vascular lesions. Besides their role in driving chronic vascular inflammation, T_{RM} may provide important clues on pathogenic principles in inflammatory vasculopathies. In the vascular tree, GCA is characterized by stringent tissue tropism. Parameters defining the susceptibility of certain arteries to the disease, while others are protected, have not been identified. The ascending aorta, the aortic arch, the distal subclavian arteries, and the temporal arteries are particularly susceptible. Considering the critical role of T_{RM} in driving persistent inflammation, the local microenvironment may dictate the survival of T_{RM}. In this model, nonpermissive microenvironments would protect the immunoprivilege of many arterial walls by failing to support the persistence of tissue-residing T_{RM}. Molecular definition of such microenvironmental niches could greatly enhance our understanding of the disease process.

In conclusion, persistence of vessel wall inflammation in medium and large vessels appears to be dependent on a small population of highly specialized T-cells, characterized by their ability to survive in the tissue microenvironment. The longevity of such $CD4^+CD103^+$ T_{RM} requires cytokine signals that are mediated through the common γ-chain; rendering such T_{RM} susceptible to kinase inhibitors that can disrupt γ-chain–dependent signaling. Depletion of such $CD4^+CD103^+$ T_{RM} was sufficient to inhibit a cascade of pathogenic events: the production of effector cytokines (IFN-γ, IL-17 and IL-21), the formation of inflammation-induced

microvascular networks and the expansion of the intimal layer. The JAK inhibitor tested here is approved for treatment of patients with rheumatoid arthritis and has been shown to have acceptable toxicity risks[50]. Targeting dysregulated T-cells instead of suppressing innate immunity (e.g. through corticosteroids) promises to fulfill a gap in the management of patients with vasculitis, while also providing informative insights into basic immune abnormalities of patients with aortitis and medium-vessel vasculitis.

Acknowledgments

HZ, RW, JJG and CMW designed the research; HZ, RW performed all experiments; GB contributed expertise in case identification and tissue analysis; all authors analyzed data; CMW, HZ and JJG wrote the paper.

Sources of Funding

This work was supported by the National Institutes of Health (R01 AR042547, R01 HL117913, R01 AI108906 and P01 HL129941 to CMW and R01 AI108891, R01 AG045779 and I01 BX001669 to JJG) and the Govenar Discovery Fund.

Disclosures

This work was partially supported by a Sponsored Research Agreement from Pfizer, Inc.

References

1. Weyand CM and Goronzy JJ. Medium- and large-vessel vasculitis. *N Engl J Med*. 2003;349:160-9.

2. Maleszewski JJ, Younge BR, Fritzlen JT, Hunder GG, Goronzy JJ, Warrington KJ and Weyand CM. Clinical and pathological evolution of giant cell arteritis: a prospective study of follow-up temporal artery biopsies in 40 treated patients. *Mod Pathol*. 2017;30 788-796.
3. Carmona FD, Vaglio A, Mackie SL, Hernandez-Rodriguez J, Monach PA, Castaneda S, Solans R, Morado IC, Narvaez J, Ramentol-Sintas M, Pease CT, Dasgupta B, Watts R, Khalidi N, Langford CA, Ytterberg S, Boiardi L, Beretta L, Govoni M, Emmi G, Bonatti F, Cimmino MA, Witte T, Neumann T, Holle J, Schonau V, Sailler L, Papo T, Haroche J, Mahr A, Mouthon L, Molberg O, Diamantopoulos AP, Voskuyl A, Brouwer E, Daikeler T, Berger CT, Molloy ES, O'Neill L, Blockmans D, Lie BA, McLaren P, Vyse TJ, Wijmenga C, Allanore Y, Koeleman BP, Spanish CGAG, Consortium U, Vasculitis Clinical Research C, Barrett JH, Cid MC, Salvarani C, Merkel PA, Morgan AW, Gonzalez-Gay MA and Martin J. A Genome-wide Association Study Identifies Risk Alleles in Plasminogen and P4HA2 Associated with Giant Cell Arteritis. *Am J Hum Genet*. 2017;100:64-74.
4. Dal Canto AJ, Swanson PE, O'Guin AK, Speck SH and Virgin HW. IFN-gamma action in the media of the great elastic arteries, a novel immunoprivileged site. *J Clin Invest*. 2001;107:R15-22.
5. Tellides G and Pober JS. Inflammatory and immune responses in the arterial media. *Circ Res*. 2015;116:312-22.
6. Zhang H, Watanabe R, Berry GJ, Vaglio A, Liao YJ, Warrington KJ, Goronzy JJ and Weyand CM. Immunoinhibitory checkpoint deficiency in medium and large vessel vasculitis. *Proc Natl Acad Sci U S A*. 2017;114:E970-E979.
7. Watanabe R, Zhang H, Berry G, Goronzy JJ and Weyand CM. Immune checkpoint dysfunction in large and medium vessel vasculitis. *Am J Physiol Heart Circ Physiol*. 2017;312:H1052-H1059.
8. Terrier B, Geri G, Chaara W, Allenbach Y, Rosenzwajg M, Costedoat-Chalumeau N, Fouret P, Musset L, Benveniste O, Six A, Klatzmann D, Saadoun D and Cacoub P. Interleukin-21 modulates Th1 and Th17 responses in giant cell arteritis. *Arthritis Rheum*. 2012;64:2001-11.
9. Ciccia F, Rizzo A, Guggino G, Cavazza A, Alessandro R, Maugeri R, Cannizzaro A, Boiardi L, Iacopino DG, Salvarani C and Triolo G. Difference in the expression of IL-9 and IL-17 correlates with different histological pattern of vascular wall injury in giant cell arteritis. *Rheumatology (Oxford)*. 2015;54:1596-604.
10. Park CO and Kupper TS. The emerging role of resident memory T cells in protective immunity and inflammatory disease. *Nat Med*. 2015;21:688-97.
11. Gebhardt T, Wakim LM, Eidsmo L, Reading PC, Heath WR and Carbone FR. Memory T cells in nonlymphoid tissue that provide enhanced local immunity during infection with herpes simplex virus. *Nat Immunol*. 2009;10:524-30.
12. Lories RJ and McInnes IB. Primed for inflammation: enthesis-resident T cells. *Nat Med*. 2012;18:1018-9.
13. Watanabe R, Gehad A, Yang C, Scott LL, Teague JE, Schlapbach C, Elco CP, Huang V, Matos TR, Kupper TS and Clark RA. Human skin is protected by four functionally and phenotypically discrete populations of resident and recirculating memory T cells. *Sci Transl Med*. 2015;7:279ra39.
14. O'Shea JJ, Gadina M and Schreiber RD. Cytokine signaling in 2002: new surprises in the Jak/Stat pathway. *Cell*. 2002;109 Suppl:S121-31.

15. O'Shea JJ, Schwartz DM, Villarino AV, Gadina M, McInnes IB and Laurence A. The JAK-STAT pathway: impact on human disease and therapeutic intervention. *Annu Rev Med*. 2015;66:311-28.
16. Mullen AC, High FA, Hutchins AS, Lee HW, Villarino AV, Livingston DM, Kung AL, Cereb N, Yao TP, Yang SY and Reiner SL. Role of T-bet in commitment of TH1 cells before IL-12-dependent selection. *Science*. 2001;292:1907-10.
17. O'Shea JJ and Plenge R. JAK and STAT signaling molecules in immunoregulation and immune-mediated disease. *Immunity*. 2012;36:542-50.
18. Remmers EF, Plenge RM, Lee AT, Graham RR, Hom G, Behrens TW, de Bakker PI, Le JM, Lee HS, Batliwalla F, Li W, Masters SL, Booty MG, Carulli JP, Padyukov L, Alfredsson L, Klareskog L, Chen WV, Amos CI, Criswell LA, Seldin MF, Kastner DL and Gregersen PK. STAT4 and the risk of rheumatoid arthritis and systemic lupus erythematosus. *N Engl J Med*. 2007;357:977-86.
19. Gestermann N, Mekinian A, Comets E, Loiseau P, Puechal X, Hachulla E, Gottenberg JE, Mariette X and Miceli-Richard C. STAT4 is a confirmed genetic risk factor for Sjogren's syndrome and could be involved in type 1 interferon pathway signaling. *Genes Immun*. 2010;11:432-8.
20. Meyer DM, Jesson MI, Li X, Elrick MM, Funckes-Shippy CL, Warner JD, Gross CJ, Dowty ME, Ramaiah SK, Hirsch JL, Saabye MJ, Barks JL, Kishore N and Morris DL. Anti-inflammatory activity and neutrophil reductions mediated by the JAK1/JAK3 inhibitor, CP-690,550, in rat adjuvant-induced arthritis. *J Inflamm (Lond)*. 2010;7:41.
21. O'Shea JJ, Laurence A and McInnes IB. Back to the future: oral targeted therapy for RA and other autoimmune diseases. *Nat Rev Rheumatol*. 2013;9:173-82.
22. Degryse S, de Bock CE, Cox L, Demeyer S, Gielen O, Mentens N, Jacobs K, Geerdens E, Gianfelici V, Hulselmans G, Fiers M, Aerts S, Meijerink JP, Tousseyn T and Cools J. JAK3 mutants transform hematopoietic cells through JAK1 activation, causing T-cell acute lymphoblastic leukemia in a mouse model. *Blood*. 2014;124:3092-100.
23. Russell SM, Tayebi N, Nakajima H, Riedy MC, Roberts JL, Aman MJ, Migone TS, Noguchi M, Markert ML, Buckley RH, O'Shea JJ and Leonard WJ. Mutation of Jak3 in a patient with SCID: essential role of Jak3 in lymphoid development. *Science*. 1995;270:797-800.
24. Macchi P, Villa A, Giliani S, Sacco MG, Frattini A, Porta F, Ugazio AG, Johnston JA, Candotti F, O'Shea JJ, Vezzoni P and Notarangelo L. Mutations of Jak-3 gene in patients with autosomal severe combined immune deficiency (SCID). *Nature*. 1995;377:65-8.
25. Schindler CW. Series introduction. JAK-STAT signaling in human disease. *J Clin Invest*. 2002;109:1133-7.
26. Cid MC, Cebrian M, Font C, Coll-Vinent B, Hernandez-Rodriguez J, Esparza J, Urbano-Marquez A and Grau JM. Cell adhesion molecules in the development of inflammatory infiltrates in giant cell arteritis: inflammation-induced angiogenesis as the preferential site of leukocyte-endothelial cell interactions. *Arthritis Rheum*. 2000;43:184-94.
27. Mitchell EB and Cestari DM. Giant cell arteritis and angiogenesis: a review. *Semin Ophthalmol*. 2009;24:190-3.
28. Koster MJ, Matteson EL and Warrington KJ. Recent advances in the clinical management of giant cell arteritis and Takayasu arteritis. *Curr Opin Rheumatol*. 2016;28:211-7.
29. Buttgereit F, Dejaco C, Matteson EL and Dasgupta B. Polymyalgia Rheumatica and Giant Cell Arteritis: A Systematic Review. *JAMA*. 2016;315:2442-58.

30. Piggott K, Deng J, Warrington K, Younge B, Kubo JT, Desai M, Goronzy JJ and Weyand CM. Blocking the NOTCH pathway inhibits vascular inflammation in large-vessel vasculitis. *Circulation*. 2011;123:309-18.
31. Wen Z, Shen Y, Berry G, Shahram F, Li Y, Watanabe R, Liao YJ, Goronzy JJ and Weyand CM. The microvascular niche instructs T cells in large vessel vasculitis via the VEGF-Jagged1-Notch pathway. *Sci Transl Med*. 2017;9:eaal3322.
32. Yang Z, Shen Y, Oishi H, Matteson EL, Tian L, Goronzy JJ and Weyand CM. Restoring oxidant signaling suppresses proarthritogenic T cell effector functions in rheumatoid arthritis. *Sci Transl Med*. 2016;8:331ra38.
33. Dowty ME, Jesson MI, Ghosh S, Lee J, Meyer DM, Krishnaswami S and Kishore N. Preclinical to clinical translation of tofacitinib, a Janus kinase inhibitor, in rheumatoid arthritis. *J Pharmacol Exp Ther*. 2014;348:165-73.
34. Calama E, Ramis I, Domenech A, Carreno C, De Alba J, Prats N and Miralpeix M. Tofacitinib ameliorates inflammation in a rat model of airway neutrophilia induced by inhaled LPS. *Pulm Pharmacol Ther*. 2017;43:60-67.
35. Weyand CM, Hicok KC, Hunder GG and Goronzy JJ. Tissue cytokine patterns in patients with polymyalgia rheumatica and giant cell arteritis. *Ann Intern Med*. 1994;121:484-91.
36. Deng J, Younge BR, Olshen RA, Goronzy JJ and Weyand CM. Th17 and Th1 T-cell responses in giant cell arteritis. *Circulation*. 2010;121:906-15.
37. Weyand CM, Younge BR and Goronzy JJ. IFN-gamma and IL-17: the two faces of T-cell pathology in giant cell arteritis. *Curr Opin Rheumatol*. 2011;23:43-9.
38. Darnell JE, Jr. STATs and gene regulation. *Science*. 1997;277:1630-5.
39. Murray PJ. The JAK-STAT signaling pathway: input and output integration. *J Immunol*. 2007;178:2623-9.
40. Watanabe R, Hosgur E, Zhang H, Wen Z, Berry G, Goronzy JJ and Weyand CM. Pro-inflammatory and anti-inflammatory T cells in giant cell arteritis. *Joint Bone Spine*. 2016;84:421-426.
41. Masopust D, Vezys V, Wherry EJ, Barber DL and Ahmed R. Cutting edge: gut microenvironment promotes differentiation of a unique memory CD8 T cell population. *J Immunol*. 2006;176:2079-83.
42. Cepek KL, Parker CM, Madara JL and Brenner MB. Integrin alpha E beta 7 mediates adhesion of T lymphocytes to epithelial cells. *J Immunol*. 1993;150:3459-70.
43. Adachi T, Kobayashi T, Sugihara E, Yamada T, Ikuta K, Pittaluga S, Saya H, Amagai M and Nagao K. Hair follicle-derived IL-7 and IL-15 mediate skin-resident memory T cell homeostasis and lymphoma. *Nat Med*. 2015;21:1272-9.
44. Makkuni D, Bharadwaj A, Wolfe K, Payne S, Hutchings A and Dasgupta B. Is intimal hyperplasia a marker of neuro-ophthalmic complications of giant cell arteritis? *Rheumatology (Oxford)*. 2008;47:488-90.
45. Wen Z, Shimojima Y, Shirai T, Li Y, Ju J, Yang Z, Tian L, Goronzy JJ and Weyand CM. NADPH oxidase deficiency underlies dysfunction of aged CD8+ Tregs. *J Clin Invest*. 2016;126:1953-67.
46. Meraz MA, White JM, Sheehan KC, Bach EA, Rodig SJ, Dighe AS, Kaplan DH, Riley JK, Greenlund AC, Campbell D, Carver-Moore K, DuBois RN, Clark R, Aguet M and Schreiber RD. Targeted disruption of the Stat1 gene in mice reveals unexpected physiologic specificity in the JAK-STAT signaling pathway. *Cell*. 1996;84:431-42.

47. Park C, Li S, Cha E and Schindler C. Immune response in Stat2 knockout mice. *Immunity*. 2000;13:795-804.
48. Kaiser M, Younge B, Bjornsson J, Goronzy JJ and Weyand CM. Formation of new vasa vasorum in vasculitis. Production of angiogenic cytokines by multinucleated giant cells. *Am J Pathol*. 1999;155:765-74.
49. Ciccia F, Alessandro R, Rizzo A, Raimondo S, Giardina A, Raiata F, Boiardi L, Cavazza A, Guggino G, De Leo G, Salvarani C and Triolo G. IL-33 is overexpressed in the inflamed arteries of patients with giant cell arteritis. *Ann Rheum Dis*. 2013;72:258-64.
50. Winthrop KL. The emerging safety profile of JAK inhibitors in rheumatic disease. *Nat Rev Rheumatol*. 2017;13:320.

Table 1. Clinical characteristics of patients with GCA

Parameters	Patients (n = 54)
Age (year, mean ± SD)	70.87 ± 8.7
Female	38/54
Ethnicity	
Caucasian	47
Hispanic	4
Asian	2
African-American	1
Disease duration (month, mean ± SD)	6.0 ± 9.55
ESR (mean ± SD, mm/h)	52.09±26.02
CRP (mean ± SD, mg/dL)	8.93±10.64
Aortic/large vessel involvement	23/54
Polymyalgia rheumatica	30/54
Untreated	19/54
Prednisone (mg/day, mean ± SD)	12.07±14.3

Figure Legends

Figure 1. Expression profiles of STAT family transcription factors and their respective target genes in arteries affected by GCA. Temporal artery biopsies were categorized according to histology into those free of vasculitis and those with classical findings of giant cell arteritis (GCA). Tissue extracts were processed for gene expression profiling applying RT-PCR and expression levels for individual genes were adjusted to β-actin. (A) Expression levels of selected target genes for each of the STAT family members shown as a heat map. Each lane represents one arterial sample. (B-G) Expression levels for transcription factors of the STAT family. (H-J) Tissue transcript concentrations for type I (IFN-α, IFN-β) and type II interferon (IFN-γ). Data from 8 vasculitis-free and 8 GCA-affected arteries were compared by Wilcoxon test and are presented as mean ± SEM. **P*<0.05, ***P*<0.01, ***<0.001.

Figure 2. CD4 effector T-cells from GCA patients are sensitive to JAK-STAT inhibition. Peripheral blood $CD4^+$ T-cells from GCA patients and age-matched healthy controls (HC) were stimulated with anti-CD3/CD28 in the absence or presence of the jakinib tofacitinib (10 nM; 30 nM). On day 6, intracellular IFN-γ was analyzed by flow cytometry. Fluorescence minus one (FMO) and isotype control were used as controls. (A) Representative dot blots. (B) Frequencies of IFN-γ^+ $CD4^+$ T-cells. Mean ± SEM from 12 healthy controls and 12 patients. One way ANOVA and pair-wise comparison using Tukey's method to adjust for multiple testing was applied. **P*<0.05, ****P*<0.001.

Figure 3. Tofacitinib suppresses T-cell expansion in the vasculitic lesions. NSG mice engrafted with human medium-sized arteries were immunoreconstituted with PBMCs from GCA patients as in Suppl. Fig. 1. Vasculitic lesions accumulate within the human artery within 7-10 days. Subsequently, chimeric mice were treated with tofacitinib (3 mg/kg orally/day) or vehicle for one week. mRNA was prepared from explanted arteries for gene expression profiling (RT-PCR). Tissue sections were analyzed by H&E staining and immunohistochemistry (IHC). Tissue-residing cells were extracted from digested tissue. Each point represents one artery, paired arteries are line-connected. (A) Representative H&E stains from explanted arteries (600×). (B) IHC staining for $CD3^+$ T-cells in the tissue sections (600×). (C) Density of the T-cell infiltrates measured by either quantification of TCR transcripts or enumeration of $CD3^+$ cells by IHC (paired Wilcoxon test). (D) Tissue macrophage density estimated by CD163 transcript quantification (paired Wilcoxon test) (E, F) Proliferating T-cells ($CD3^+Ki\text{-}67^+$) in the vasculitic lesions detected by dual-color staining. Representative images (scale bar: 200 μm) and $CD3^+Ki\text{-}67^+$ cell percentages (compared by t- test). (G, H) $CD4^+CD103^+$ tissue-resident memory T-cells quantified by flow cytometry of tissue-extracted cells. Representative dot blots and absolute numbers per 100 mg of arterial tissue (p by t-test). $^{**}P<0.01$.

Figure 4. Tofacitinib suppresses multiple vasculitogenic effector T-cell lineages. Vasculitis was induced in human arteries and chimeric mice were treated with vehicle or tofacitinib as in Figure 3. Gene expression of transcription factors (A-D) and T-cell effector cytokines (E-G) was quantified by RT-PCR of tissue-extracted mRNA. Each data point represents one artery and paired arteries are connected by a line. $^{**}p<0.01$ by paired Wilcoxon test. ns: not significant.

Comparisons of T-bet, RORC, BCL-6, IFN-γ, IL-17 and IL-21 are statistically significant after controlling the family-wise error rate at the 0.05 level using Hochberg's step-down adjustment.

Figure 5. Tofacitinib shortens the survival of tissue-resident memory T-cells. Vasculitis was induced in engrafted human arteries as in Figure 3. After vasculitis induction, arteries were transengrafted into an "empty" NSG mouse. Chimeras with arteries from the same donor were assigned to parallel treatment arms: oral tofacitinib (3 mg/kg/day) or vehicle for 7 days. Explanted arteries were sectioned for H&E and immunofluorescence staining, or tissue-residing cells were extracted from digested explants and mRNA was extracted for transcriptome analysis by RT-PCR (n=8 arteries). (A) Scheme of the animal experiments. (B) H&E sections from pretransengraftment and posttransengraftment arteries. Representative images (scale bar: 200 μm). (C) Representative IHC images from pretransengraftment and posttransengraftment arteries stained with anti-CD3. (D) T cell numbers in tissue sections compared by paired Wilcoxon test. (E, F) Proliferating $CD3^+Ki\text{-}67^+$ T-cells in transengrafted arteries. Representative images and frequency of $Ki\text{-}67^+$ T-cells. (G, H) Flow cytometry of tissue-extracted $CD4^+CD103^+$ tissue-resident memory T-cells. Representative dot blots and frequencies (t-test performed). (I) Gene expression profiling in arterial grafts before and after transengraftment assessed by RT-PCR. $^{**}p<0.01$ by paired Wilcoxon testing. Comparisons of TCR, T-bet, RORC, IFN-γ, IL-17 and IL-21 remain statistically significant after controlling the family-wise error rate at the 0.05 level using Hochberg's step-down adjustment.

Figure 6. Tofacitinib inhibits inflammation-associated microangiogenesis. Human artery-SCID chimeras were generated as in Figure 3 and treated with vehicle or tofacitinib (3

mg/kg/day) as described above. Explanted arteries were analyzed for microangiogenesis by immunofluorescence staining of α-SMA, vWF and DAPI. Gene expression was quantified by RT-PCR. (A) Representative images of α-SMA$^+$vWF$^+$ adventitial microvessels. Left: healthy medium-sized artery; middle: artery explanted from mice that did not receive human PBMCs; right: artery explanted from chimeras that were immunoreconstituted with GCA PBMCs (scale bar: 200 μm). (B) Quantification of adventitial microvessels (n=4 each; comparison by t-test). (C, D) α-SMA$^+$/vWF$^+$ microvessels in vehicle and tofacitinib-treated grafts. Representative images (scale bar: 200 μm) and microvessel density in paired arterial grafts. Paired Wilcoxon test applied. (E) Tissue gene expression of angiogenic cytokines in vehicle and tofacitinib-treated explants. Paired arterial grafts are line-connected. *P<0.05, **P<0.01, ***P<0.001 by paired Wilcoxon test.

Figure 7. Tofacitinib inhibits intimal hyperplasia. Human artery-SCID chimeras were generated as in Figure 3 and treated with vehicle or tofacitinib (3 mg/kg/day) for 2 weeks. (A) H&E staining of tissue sections from vehicle or tofacitinib-treated arteries. Representative images (100×). (B) Intimal layer thickness measured in arterial cross-sections (n=5) Data from paired grafts are connected by a line. T-test was applied. (C, D) α-SMA$^+$ and α-SMA$^-$ cells expressing the proliferation marker Ki-67 in vehicle and tofacitinib-treated arteries. (C) Effect of tofacitinib treatment on the frequencies of Ki-67$^+$ proliferating cells assessed amongst α-SMA$^+$ and α-SMA$^-$ cells. Data are from 6 paired grafts. p by paired Wilcoxon test. (D) Representative images showing intimal α-SMA$^+$/Ki-67$^+$ cells and medial α-SMA$^-$Ki-67$^+$ cells (scale bar: 200 μm). *P<0.05, **P<0.01.

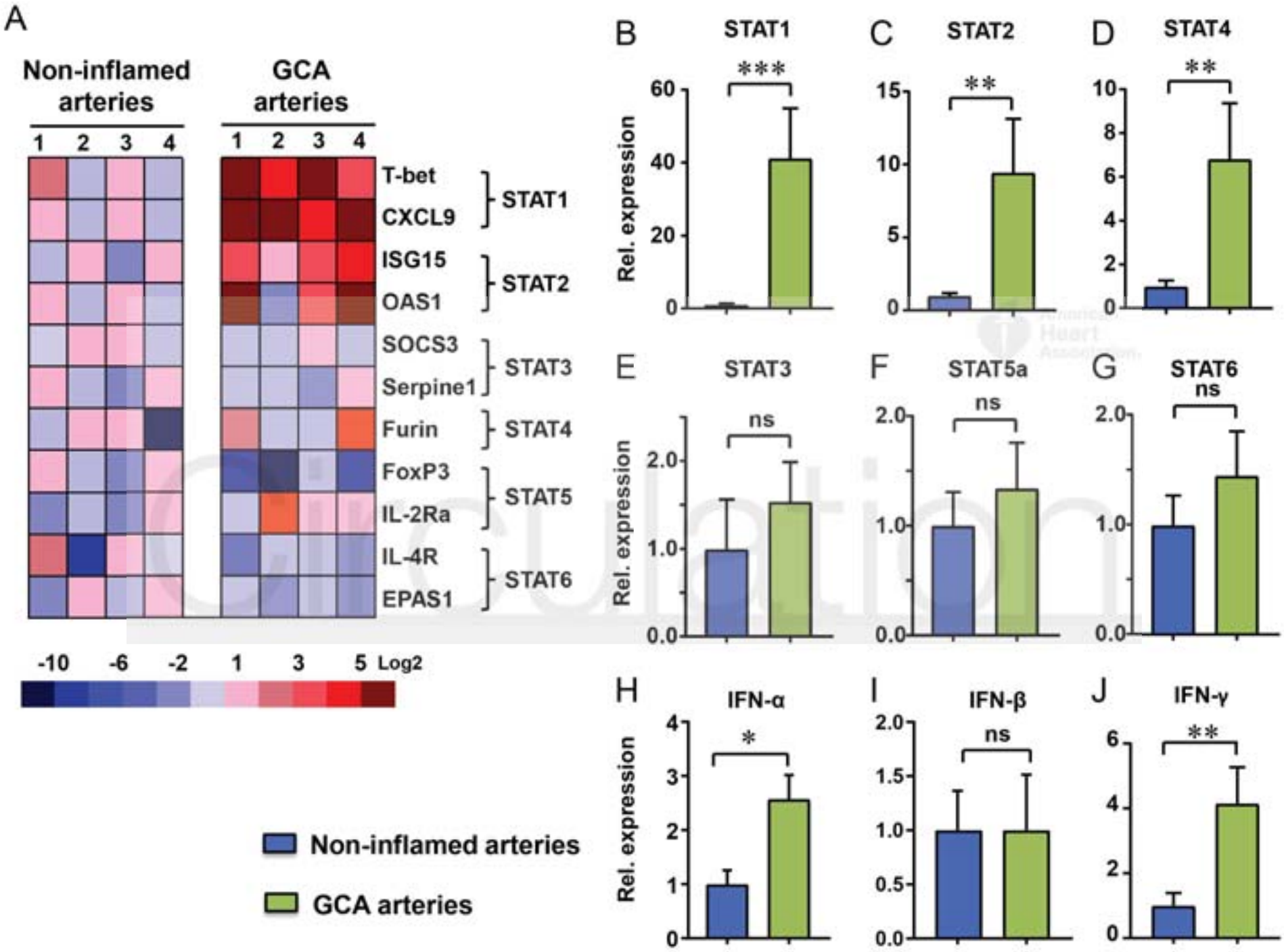
A
Non-inflamed arteries
GCA arteries
1 2 3 4
1 2 3 4
T-bet
CXCL9
ISG15
OAS1
SOCS3
Serpine1
Furin
FoxP3
IL-2Ra
IL-4R
EPAS1
STAT1
STAT2
STAT3
STAT4
STAT5
STAT6
-10 -6 -2 1 3 5 Log2
Non-inflamed arteries
GCA arteries
B STAT1
C STAT2
D STAT4
E STAT3
F STAT5a
G STAT6
H IFN-α
I IFN-β
J IFN-γ
Rel. expression
***
**
ns
*

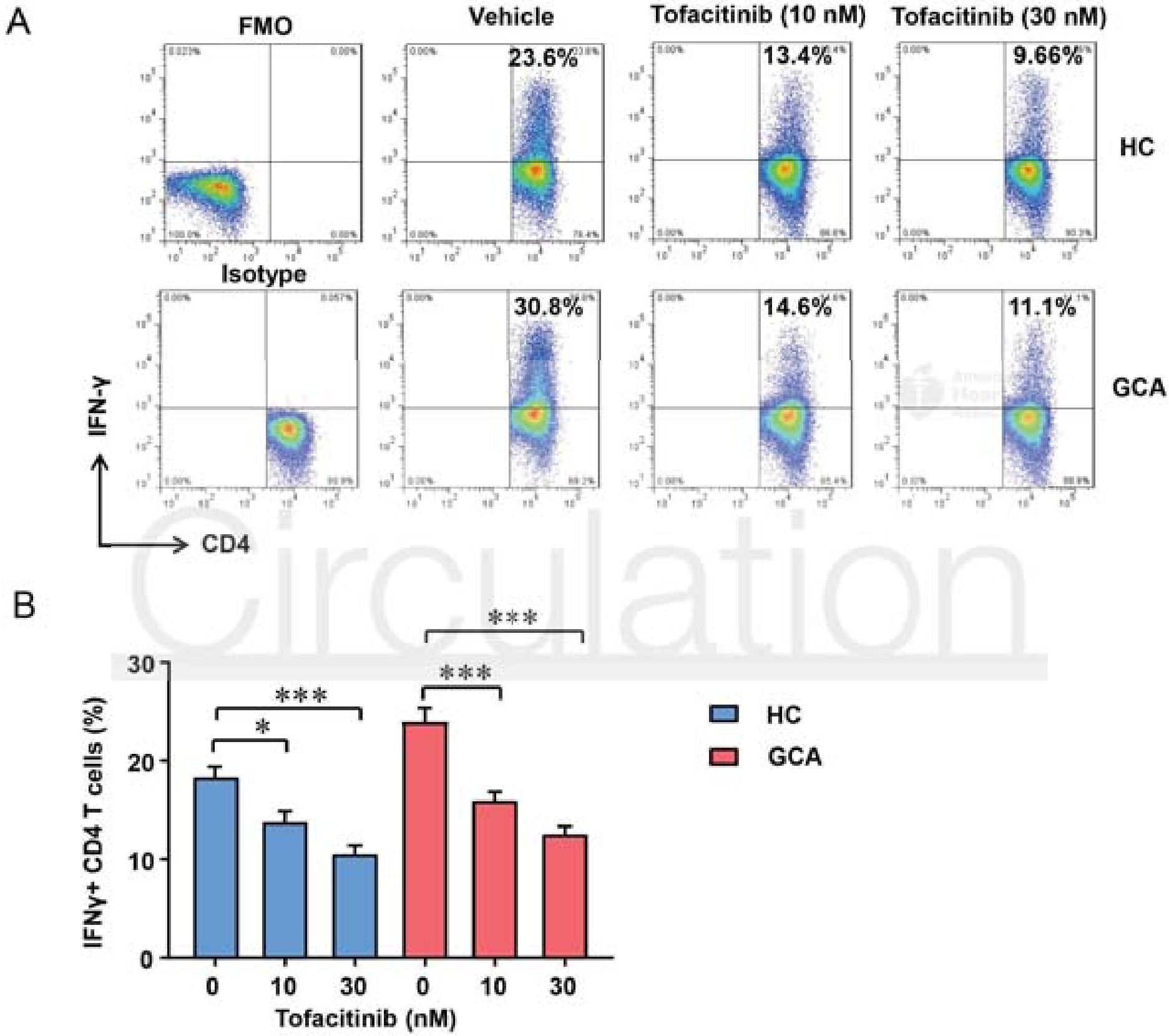
A
FMO
Vehicle
Tofacitinib (10 nM)
Tofacitinib (30 nM)
23.6%
13.4%
9.66%
HC
Isotype
30.8%
14.6%
11.1%
GCA
IFN-γ
CD4
B
***
***
***
*
IFNγ+ CD4 T cells (%)
30
20
10
0
0
10
30
0
10
30
Tofacitinib (nM)
HC
GCA

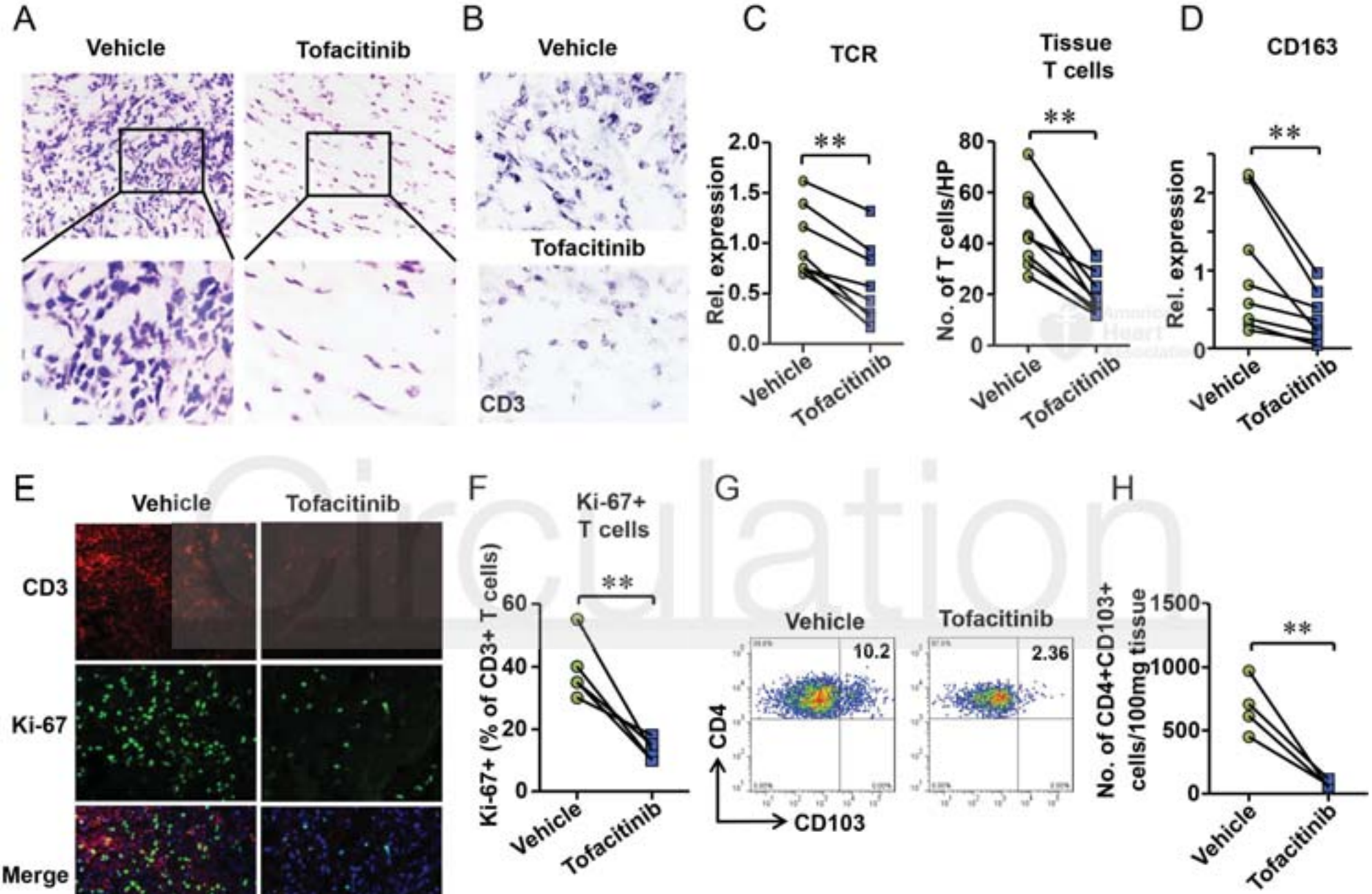
A
Vehicle
Tofacitinib
B
Vehicle
Tofacitinib
CD3
C
TCR
Rel. expression
2.0
1.5
1.0
0.5
0.0
**
Vehicle
Tofacitinib
Tissue
T cells
No. of T cells/HP
80
60
40
20
0
**
Vehicle
Tofacitinib
D
CD163
Rel. expression
2
1
0
**
Vehicle
Tofacitinib
E
Vehicle
Tofacitinib
CD3
Ki-67
Merge
F
Ki-67+
T cells
Ki-67+ (% of CD3+ T cells)
60
40
20
0
**
Vehicle
Tofacitinib
G
Vehicle
Tofacitinib
10.2
2.36
CD4
CD103
H
No. of CD4+CD103+
cells/100mg tissue
1500
1000
500
0
**
Vehicle
Tofacitinib

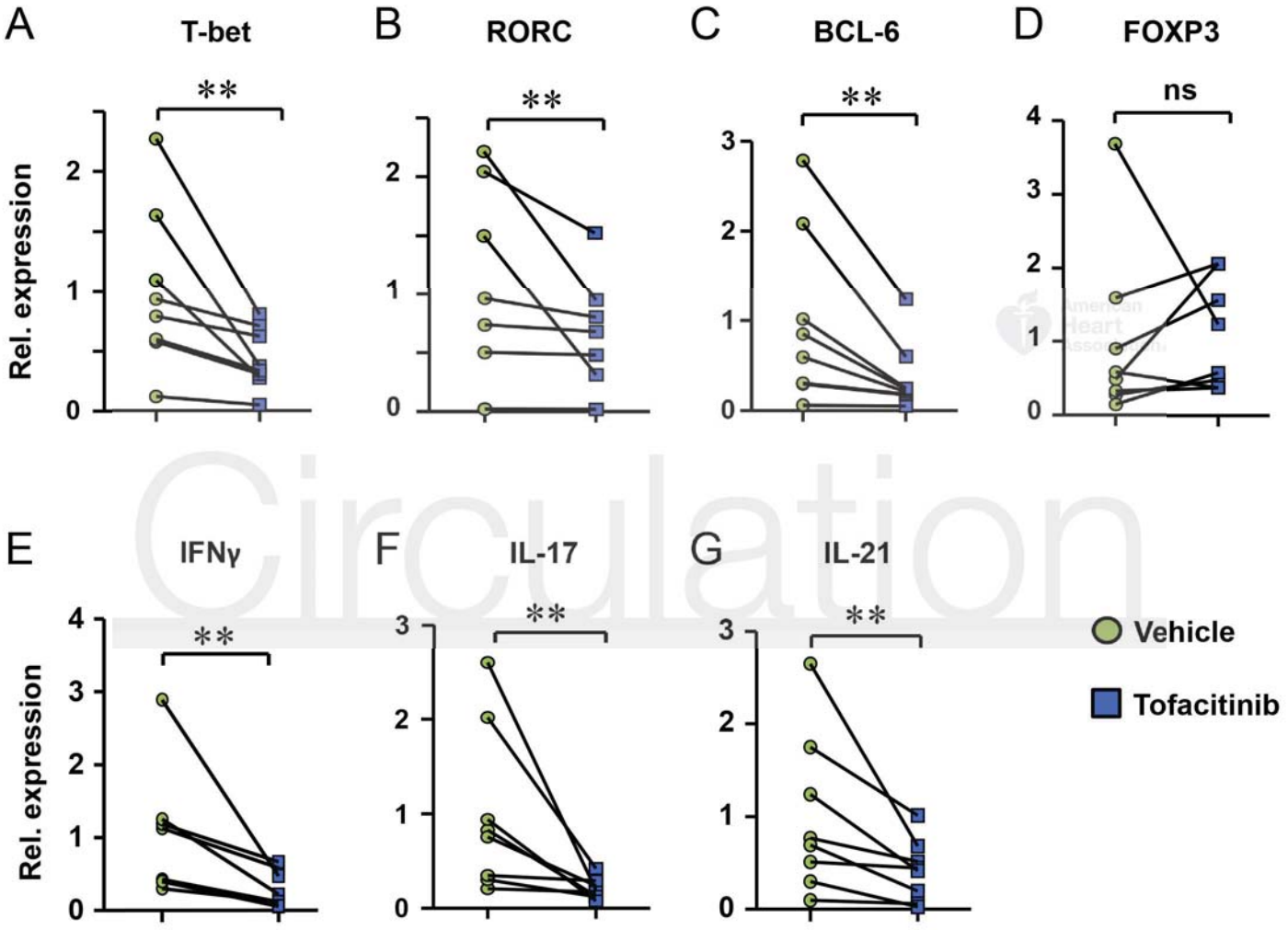

A. Scheme of the animal experiments

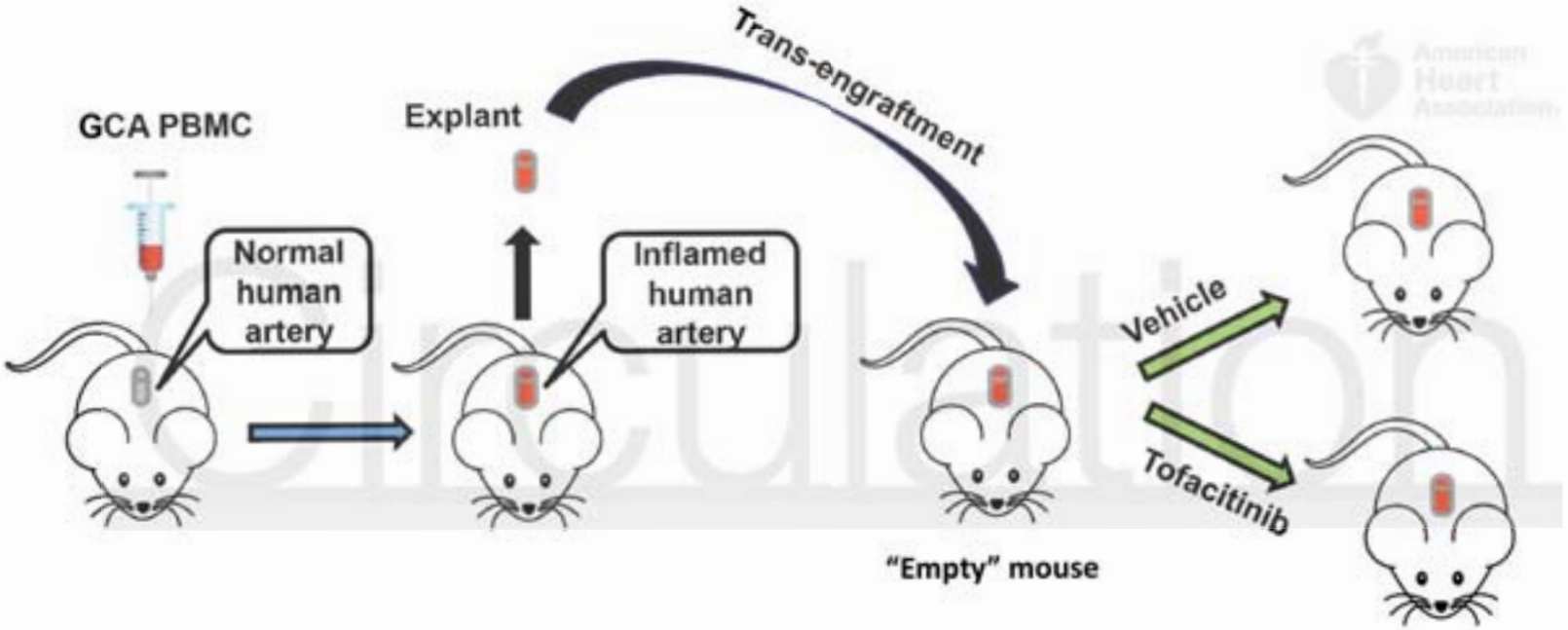

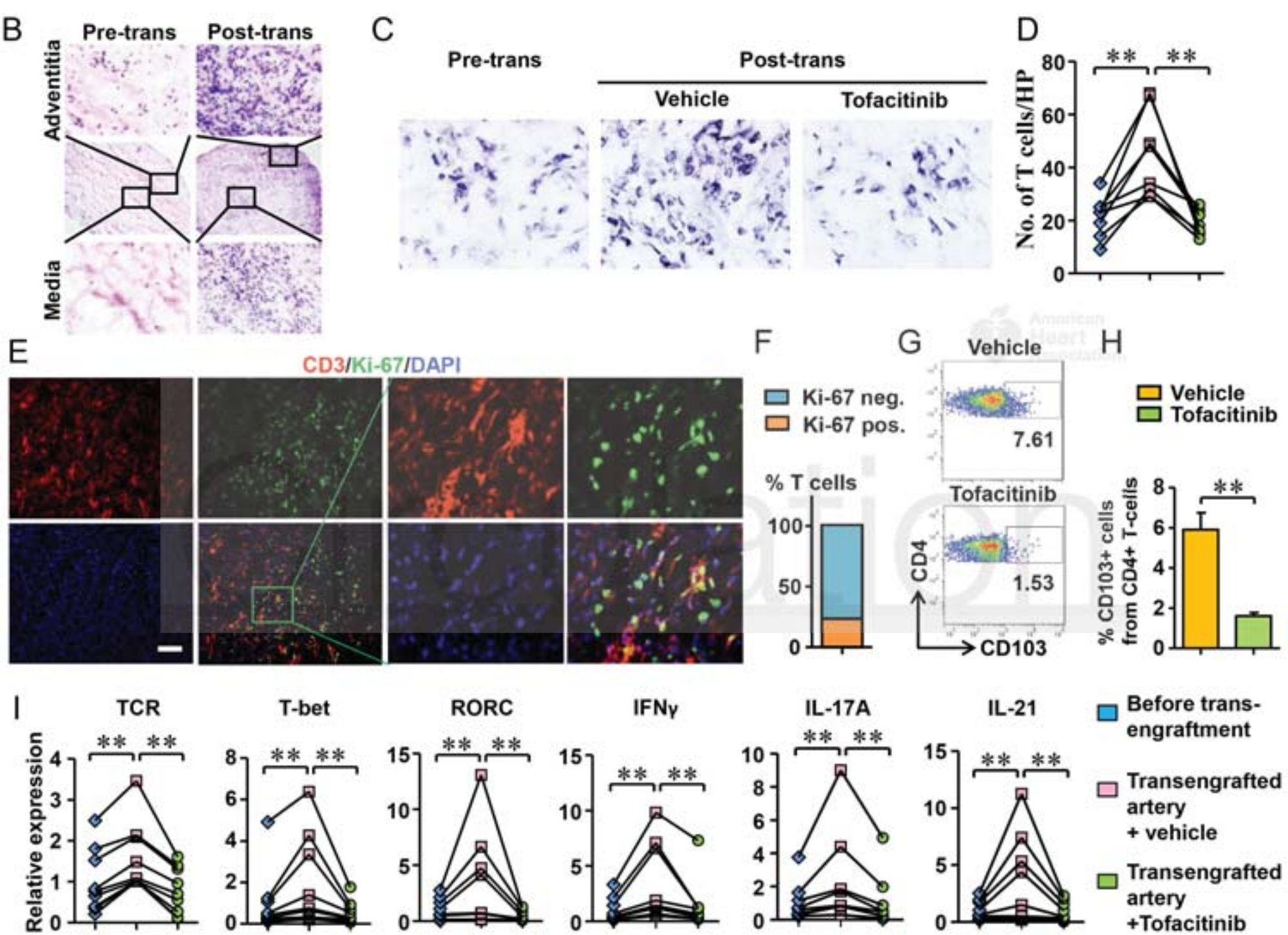
B
Pre-trans
Post-trans
Adventitia
Media
C
Pre-trans
Post-trans
Vehicle
Tofacitinib
D
No. of T cells/HP
E
CD3/Ki-67/DAPI
F
Ki-67 neg.
Ki-67 pos.
% T cells
G
Vehicle
7.61
Tofacitinib
1.53
CD4
CD103
H
Vehicle
Tofacitinib
% CD103+ cells from CD4+ T-cells
I
TCR
T-bet
RORC
IFNγ
IL-17A
IL-21
Relative expression
Before trans-engraftment
Transengrafted artery + vehicle
Transengrafted artery +Tofacitinib

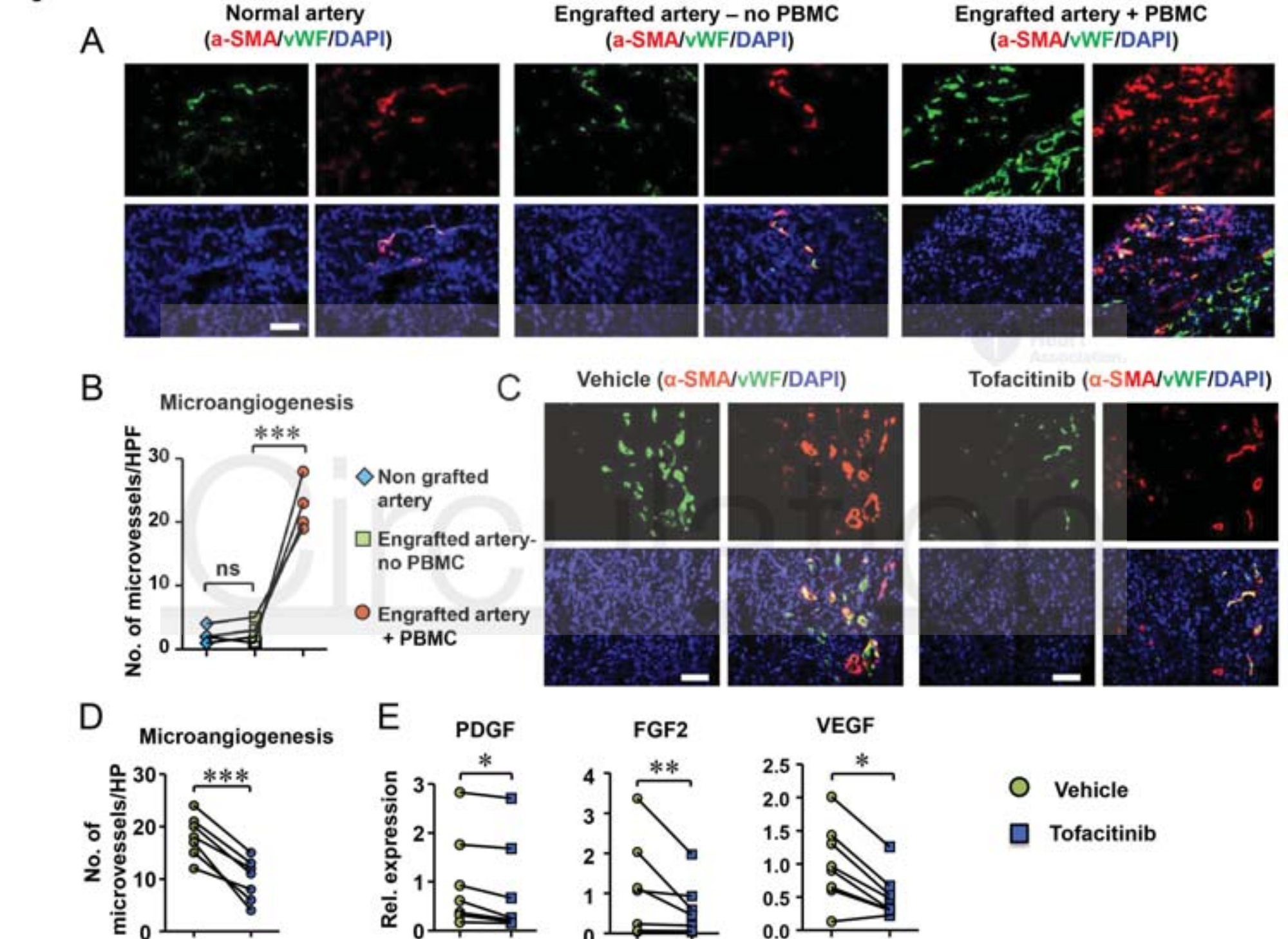
A
Normal artery
(a-SMA/vWF/DAPI)
Engrafted artery – no PBMC
(a-SMA/vWF/DAPI)
Engrafted artery + PBMC
(a-SMA/vWF/DAPI)
B
Microangiogenesis
No. of microvessels/HPF
30
20
10
0
***
ns
Non grafted artery
Engrafted artery- no PBMC
Engrafted artery + PBMC
C
Vehicle (α-SMA/vWF/DAPI)
Tofacitinib (α-SMA/vWF/DAPI)
D
Microangiogenesis
No. of microvessels/HP
30
20
10
0
***
E
PDGF
FGF2
VEGF
Rel. expression
*
**
*
Vehicle
Tofacitinib

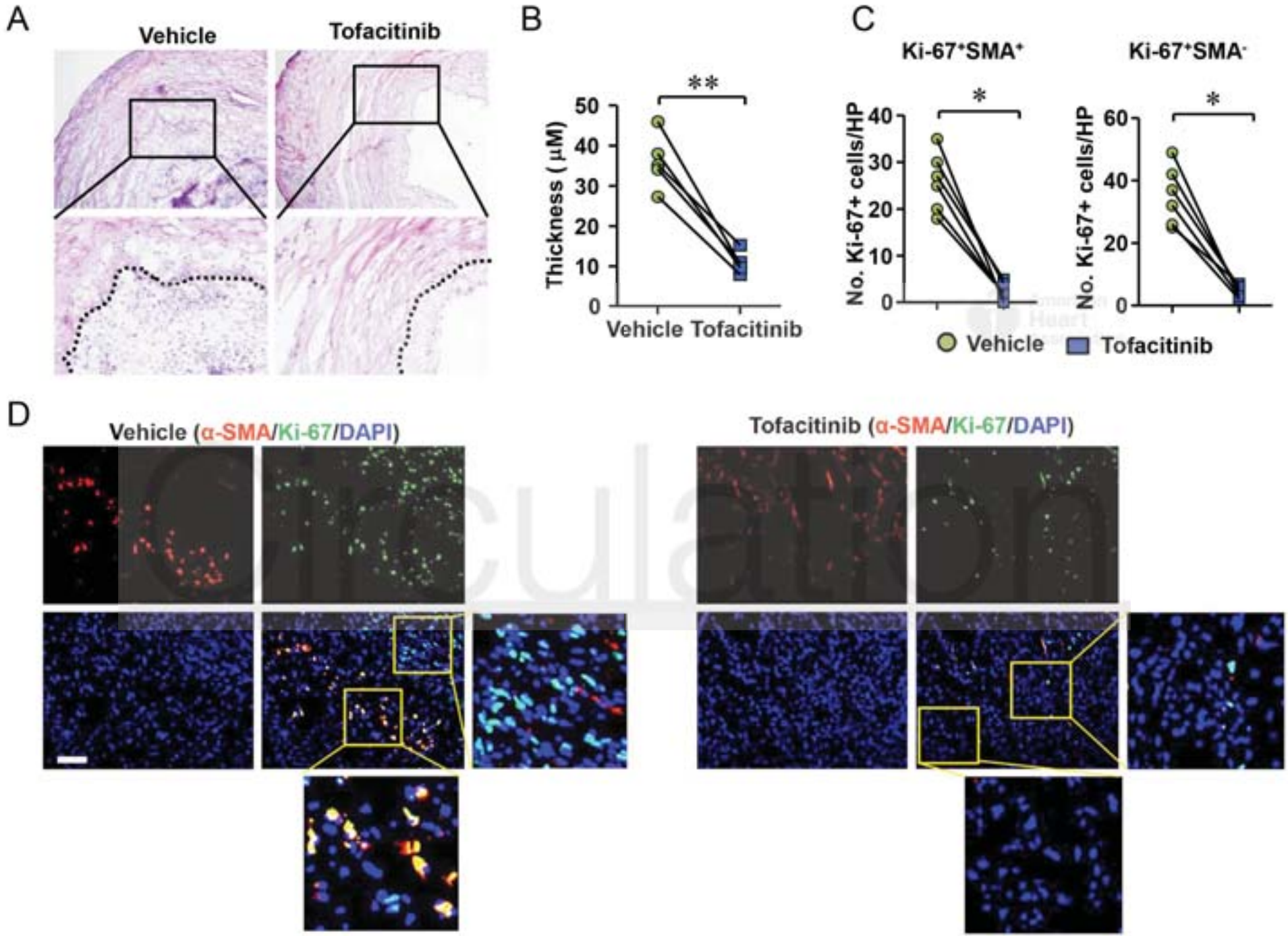
A
Vehicle
Tofacitinib
B
**
Thickness (μM)
50
40
30
20
10
0
Vehicle Tofacitinib
C
Ki-67+SMA+
Ki-67+SMA-
*
*
No. Ki-67+ cells/HP
40
30
20
10
0
No. Ki-67+ cells/HP
60
40
20
0
Vehicle
Tofacitinib
D
Vehicle (α-SMA/Ki-67/DAPI)
Tofacitinib (α-SMA/Ki-67/DAPI)

Inhibition of JAK-STAT Signaling Suppresses Pathogenic Immune Responses in Medium and Large Vessel Vasculitis

Hui Zhang, Ryu Watanabe, Gerald J. Berry, Lu Tian, Jörg J. Goronzy and Cornelia Weyand

Circulation. published online December 18, 2017;
Circulation is published by the American Heart Association, 7272 Greenville Avenue, Dallas, TX 75231

Print ISSN: 0009-7322. Online ISSN: 1524-4539

Supplementary data

Antibodies and Reagents

Anti-human CD3 PE and anti-human-CD45 APC antibodies were purchased from BD Pharmingen (San Diego, CA). The following antibodies were obtained from BioLegend (San Diego, CA): anti-human CD4 FITC, anti-human CD14 FITC, anti-human CD11c APC, anti-human CD103 PE. Rabbit anti-human CD3 and goat anti-rabbit HRP-conjugated secondary antibodies were obtained from Dako (Carpinteria, CA). Mouse anti-alpha smooth muscle actin (α-SMA), rabbit anti-von Willebrand factor (vWF), rabbit anti-Ki-67 antibodies were purchased from Abcam (Cambridge, MA). Alexa Fluor® 488 anti-rabbit and Alexa Fluor® 546 anti-mouse secondary antibodies were obtained from Life Technologies (Carlsbad, CA). Tofacitinib and vehicle were provided through a research contract with Pfizer Inc. and were administered orally at the indicated doses. Vehicle was formulated as 0.5% Methylcellulose and 2% Tween 80 in water.

Cell cultures

$CD4^+$ T-cells isolated from healthy donors or GCA patients were stimulated with anti-CD3/CD28 dynabeads in 96-well plates for 6 d. Tofacitinib (10 nM, 30 nM) or vehicle was added to the culture media on day 0. To stain for intracellular cytokines, cells were incubated with PMA (500 ng/ml), ionomycin (1 μg/ml) and BFA (1 μg/ml) for 4 h before being analyzed by flow cytometry.

Flow cytometry

Cells prepared from the blood, the murine spleen or isolated from the explanted arteries were stained with antibodies specific for CD3, CD45, CD4, CD11c, CD14,

CD103 at 4°C for 30 min. Cells were washed twice with PBS, resuspended in flow cytometry buffer and analyzed with a LSR Fortessa™ cell analyzer (BD Biosciences, Heidelberg, Germany). FlowJo (Tree Star, San Carlos, CA) software was used to analyze the data.

qPCR

RNA was isolated from tissue sections and explanted arteries and reverse-transcribed into cDNA using a reverse transcript kit following the manufacturer's instructions. A SYBR green-based quantitative RT-PCR was used to amplify cDNA. For amplification the following protocol was used: 95°C for 10 min and then 40 cycles of 95°C for 15 s 60°C for 45 s. Transcripts for individual genes were normalized to β-actin transcripts. To control for interassay variability, each value was compared to the mean values of the control group and data are presented as relative expression. PCR primers are listed in Suppl. Table 1.

Immunohistochemistry and immunofluorescence

Explanted tissues from the mice were embedded with OCT and then snapped frozen on dry ice. Tissue blocks were stored in -80°C until being used. Immunohistochemistry (IHC) or immunofluorescence was performed as previously described (2). Tissue sections were prepared at 10 microns. Sections were air dried, fixed with pre-cold acetone at 4°C for 15 min and incubated with 0.3% H_2O_2 buffer for 15 min at room temperature to remove endogenous peroxidases. CD3 antibody was used to detect T cell infiltration in the tissues. Briefly, tissues were incubated with rabbit anti-CD3 antibody at 4°C overnight. The slides were washed with PBS and incubated with HRP-conjugated goat anti-rabbit secondary antibody for 1 h at

room temperature. Specific bindings were visualized by 3, 3′ -diaminobenzidine. For immunofluorescence staining, 10 micron frozen sections were fixed with cold acetone for 15 min. Slides were washed with PBS and incubated with anti-CD3 (1:100), anti-Ki-67 (1:200), anti-αSMA (1:200), and anti-vWF (1:200) primary antibodies at 4°C overnight. Then slides were incubated with Alexa Fluor® 488 anti-rabbit (1:200), Alexa Fluor® 546 anti-mouse (1:200) secondary antibodies at room temperature for 60 min and counterstained with DAPI. Olympus fluorescence microscopy system (Olympus, Japan) was used for image acquiring.

Supplementary Figures and Figure Legends

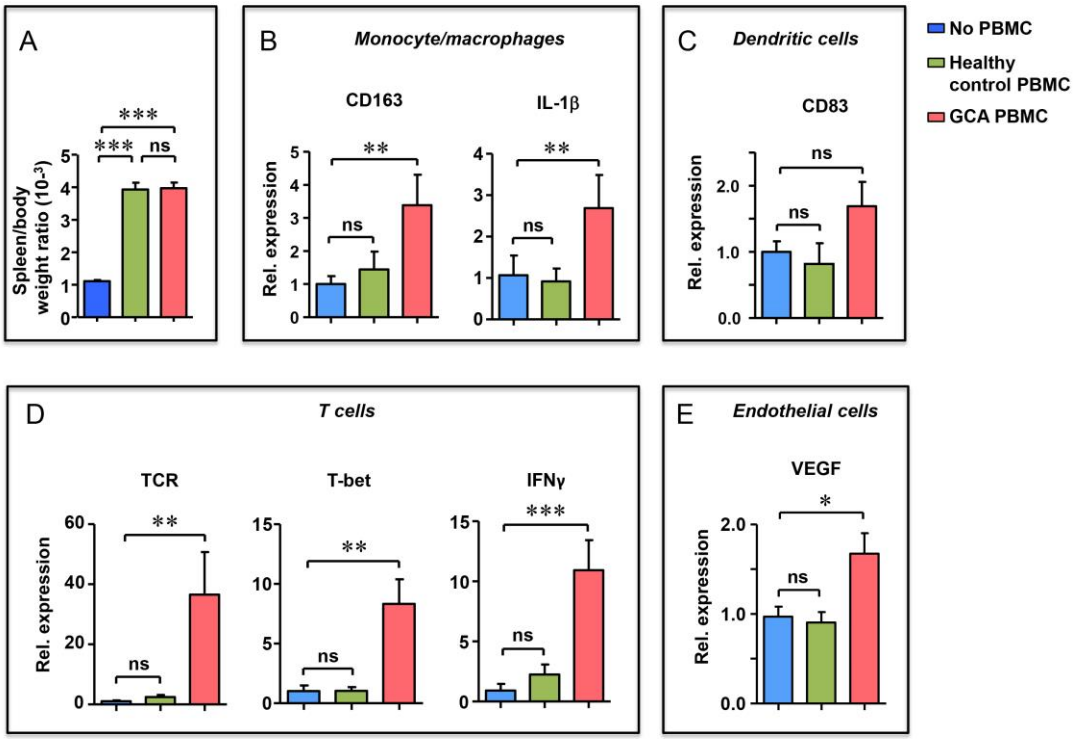

Supplementary Figure 1. GCA induced in human-artery SCID chimeric mice. Human axillary arteries were engrafted into a subcutaneous pocket placed on the midback of NSG mice. Mice received 10 µg of LPS subcutaneously 6 days after the engraftment. One to 2 days later, mice carrying arteries from the same tissue donors were assigned to one of three study arms: (1) no human peripheral blood mononuclear cells (PBMC); (2) adoptive transfer of 1×10^7 PBMC from a healthy individual; (3) adoptive transfer of 1×10^7 PBMC from a GCA patient. Seven days later, mice were sacrificed, arterial grafts were explanted and spleens harvested. (A) Spleen/body ratios of mice that had received healthy PBMCs or GCA PBMCs. (B-E) RNA was prepared from the grafts and the tissue transcriptome was assessed by RT-PCR. Data are mean ± SEM from 10 grafts in each group. ns: not significant. *p<0.05, **p<0.01, ***p<0.001 by paired Wilcoxon test. CD163, IL-1β, TCR, T-bet, IFNγ remained

statistically significant after controlling the family-wise error rate at the 0.05 level using the Hochberg's step-down adjustment.

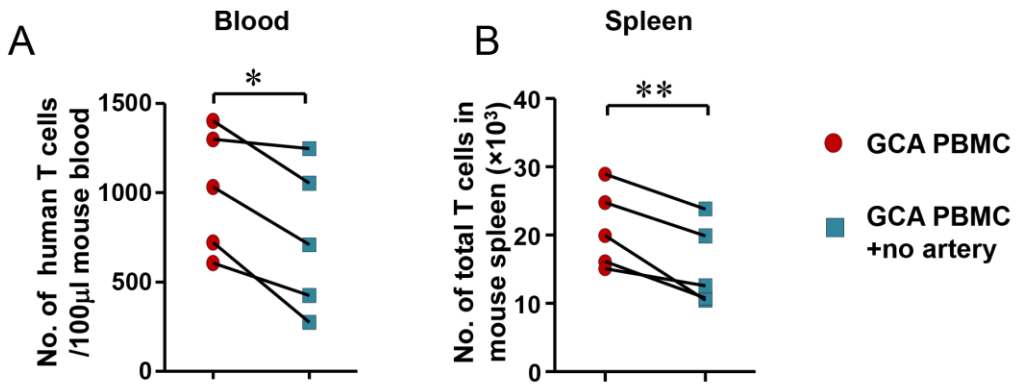

Supplementary Figure 2. Immuno-reconstitution in NSG mice in the absence or presence of transplanted human arteries. NSG mice were engrafted with human axillary arteries or sham-operated as in Suppl. Fig. 1 and adoptively transferred with 1×10^7 peripheral blood mononuclear cells (PBMC) from the same GCA patient. Seven days later, mice were sacrificed and single cell suspensions from the mouse spleen and the blood were analyzed by flow cytometry. Human T-cells were identified as $CD45^+$ $CD3^+$ cells. (A) Number of human T cells in 100 µl blood from mice engrafted with or without a human artery. (B) Number of human T cells in the spleen of mice engrafted with or without a human artery. Results from paired mice are connected by a line. The paired t-test was used. *$p<0.05$, **$p<0.01$.

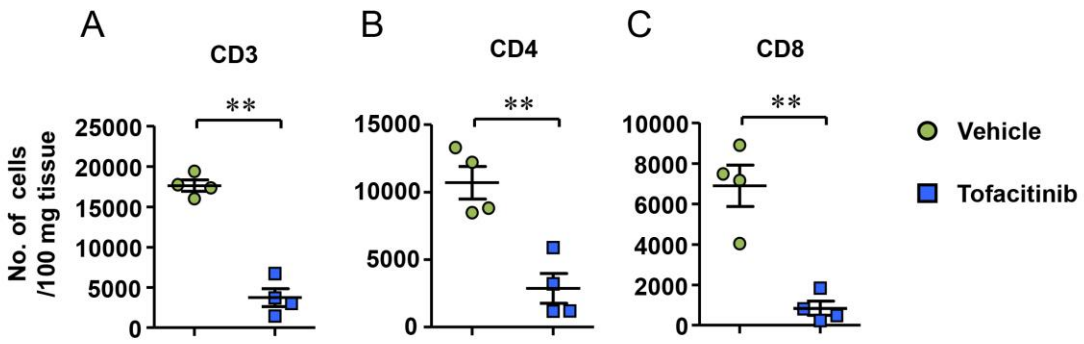

Supplementary Figure 3. Effects of tofacitinib on the density of tissue-infiltrating T-cells in human artery grafts. NSG mice were engrafted with human arteries and reconstituted with peripheral blood mononuclear cells (PBMC) from GCA patients. Chimeric mice received tofacitinib (3 mg/kg) or vehicle for 7 d. (A-C) Arterial grafts were harvested and digested. Single cell suspensions were prepared and analyzed by flow cytometry. Shown are numbers of $CD3^+$, $CD4^+$, $CD8^+$ T-cells per 100 mg tissue. Each dot represents one artery. **$p<0.01$ by t-test.

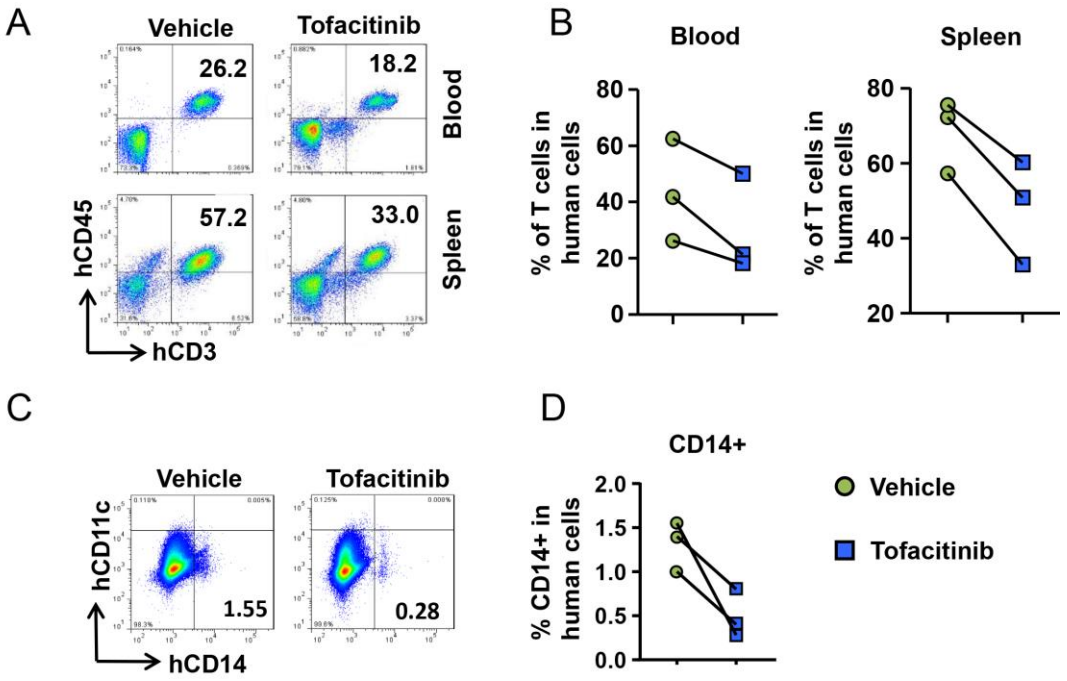

Supplementary Figure 4. **Tofacitinib inhibits in vivo expansion of T cells and monocytes.** NSG mice were reconstituted with peripheral blood mononuclear cells (PBMC) from GCA patients as in Suppl. Fig. 1 and treated daily with one oral dose of tofacitinib (3 mg/kg) or vehicle for 7 d. Single cell suspensions from the mouse spleen and the blood were analyzed by flow cytometry to identify human $CD45^+CD3^+$ T cells and human $CD45^+CD14^+$ monocytes. (A, B) Representative dot blots and frequencies of human T-cells measured in the blood and in the spleen in 3 experiments. (C, D) Representative dot blots of human $CD14^+$ monocytes in the blood. Frequencies quantified in 3 experiments.

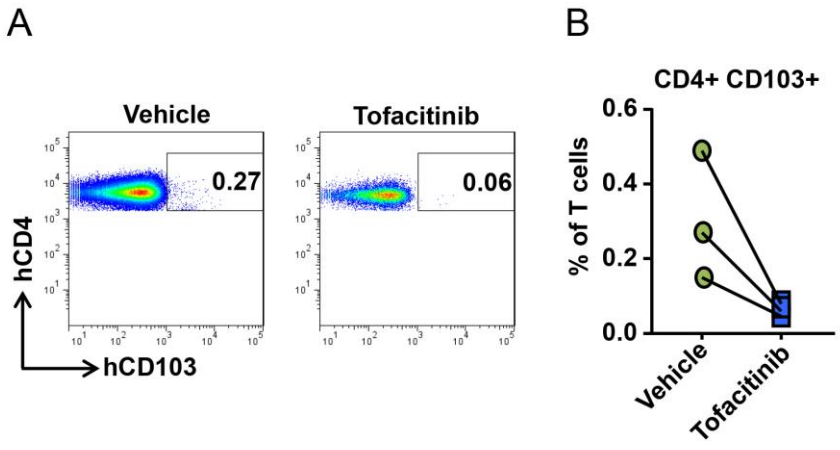

Supplementary Figure 5. Low frequency of $CD4^+CD103^+$ T-cells in the circulating blood. NSG mice were reconstituted with peripheral blood mononuclear cells (PBMC) from GCA patients as in Suppl. Fig. 1 and treated daily with one oral dose of tofacitinib (3 mg/kg) or vehicle for 7 d. Single cell suspensions from the mouse blood were analyzed by flow cytometry to identify human $CD4^+CD103^+$ T-cells. (A, B) Circulating $CD4^+CD103^+$ T cells. Representative dot blots and frequencies amongst human $CD3^+$ T-cells in 3 experiments.

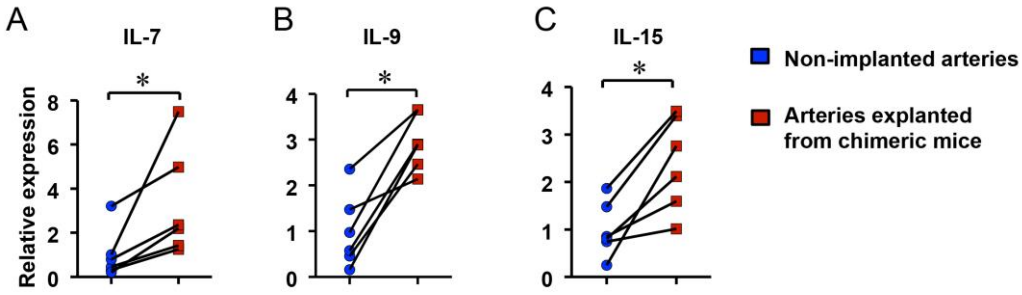

Supplementary Figure 6. **T-cell growth factors in inflamed human arteries**. NSG mice were engrafted with human arteries and reconstituted with peripheral blood mononuclear cells (PBMC) from GCA patients as described in Suppl. Fig. 1. Two weeks later, arteries were harvested. RNA was extracted from non-implanted and explanted arteries. (A-C) Concentrations of transcripts specific for IL-7, IL-9 and IL-15 were measured by RT-PCR. Each point indicates results from one artery and paired samples are connected by a line. *$p<0.05$ by paired Wilcoxon test.

Supplementary Table 1. Primers used in the manuscript

Genes	Forward primers	Reverse primers
TCR	CCTTCAACAACAGCATTATTATTCCAG	CGAGGGAGCACAGGCTGTCTTA
T-bet	TGACCCAGATGATTGTGCTCCAGT	AATCTCGGCATTCTGGTAGGCAGT
RORC	GAGAGCTAGGTGCAGAGCTT	AACTTGACAGCATCTCGGGAC
BCL-6	GTGACAAGGCCAGCAAAGAAG	GCTCTGTGGACTAACCAGACC
Foxp3	TTCAAGTTCCACAACATGCGACCC	GCACAAAGCACTTGTGCAGACTCA
IFN-γ	ACTAGGCAGCCAACCTAAGCAAGA	CATCAGGGTCACCTGACACATTCA
IL-17A	AACCGATCCACCTCACCTTGGAAT	TTCATGTGGTAGTCCACGTTCCCA
IL-7	AGAGGAACCAGCTGCAGAGA	CAAGGATCAGGGGAGGAAGT
IL-9	GGGATCCTGGACATCAACTTC	GAAGCATGGTCTGGTGCAGTT
IL-15	GAAGCCAACTGGGTGAATGT	TACTTGCATCTCCGGACTCA
IL-21	TCCTGGCAACATGGAGAGGATTGT	AGCTGGCAGAAATTCAGGGACCAA
STAT1	TCCCGGGAAGGGGCCATCAC	CGCATGGAAGTCAGGTTCGCCT
STAT2	AAGACCAGAACTGGCAGGAAG	TCTCAGCCAACTGGGTAGGAT
STAT3	CCCATACCTGAAGACCAAGTTTAT	AAGGTGAGGGACTCAAACTGC
STAT4	TTCTCCTAGGGACTGTGAGGG	GCTGCCTCCCAGTCTTGATTT
STAT5	AGTGGTCCCTGAGTTTGTGAA	GGAGTCAAGACTGTCCATTGGT
CD68	TCTTTGGGCAAAGTTTCTCCTGCC	TGCAGAAAGCAATAAGCACCAGGG
PDGF	GCAAGACCAGGACGGTCATTT	GGCACTTGACACTGCTCGT
FGF2	AGTGTGTGCTAACCGTTACCT	ACTGCCCAGTTCGTTTCAGTG
VEFG	AGGGCAGAATCATCACGAAGT	AGGGTCTCGATTGGATGGCA
CXCL9	TCGGTTAGTGGTGGAAGCATGATTG	AGACGTTCGGGTGGGATCTC
ISG15	CGCAGATCACCCAGAAGATCG	TTCGTCGCATTTGTCCACCA
OAS1	TGTCCAAGGTGGTAAAGGGTG	CCGGCGATTTAACTGATCCTG
Serpine 1	ACCGCAACGTGGTTTTCTCA	TTGAATCCCATAGCTGCTTGAAT
Furin	CCTGGTTGCTATGGGTGGTAG	AAGTGGTAATAGTCCCCGAAGA
IL-2R alpha	GACGATGACCCGCCA	CCTGGACGCACTGATAAT
EPAS1	CGGAGGTGTTCTATGAGCTGG	AGCTTGTGTGTTCGCAGGAA

IL-4R	CGTGGTCAGTGCGGATAACTA	TGGTGTGAACTGTCAGGTTTC
SOCS3	TTGAGCCGGCCCCTCTCCTC	CCAGGTGGCCGTTGACGGTC
β-actin	GATCATTGCTCCTCCTGAGC	CGTCATACTCCTGCTTGCTG